JGR Biogeosciences

RESEARCH ARTICLE
10.1029/2020JG006009

Tussocks Enduring or Shrubs Greening: Alternate Responses to Changing Fire Regimes in the Noatak River Valley, Alaska

B. V. Gaglioti[1,2], L. T. Berner[3], B. M. Jones[1], K. M. Orndahl[3], A. P. Williams[2], L. Andreu-Hayles[2], R. D. D'Arrigo[2], S. J. Goetz[3], and D. H. Mann[4]

[1]Water and Environmental Research Center, Institute of Northern Engineering, University of Alaska Fairbanks, Fairbanks, AK, USA, [2]Lamont-Doherty Earth Observatory of Columbia University, Palisades, NY, USA, [3]School of Informatics, Computing, and Cyber Systems, Northern Arizona University, Flagstaff, AZ, USA, [4]Department of Geosciences, University of Alaska Fairbanks, Fairbanks, AK, USA

Abstract As the Arctic warms, tundra wildfires are expected to become more frequent and severe. Assessing how the most flammable regions of the tundra respond to burning can inform us about how the rest of the Arctic may be affected by climate change. Here we describe ecosystem responses to tundra fires in the Noatak River watershed of northwestern Alaska using shrub dendrochronology, active-layer depth monitoring, and remotely sensed vegetation productivity. Results show that relatively productive tundra is more likely to experience fires and to burn more severely, suggesting that fuel loads currently limit tundra fire distribution in the Noatak Valley. Within three years of burning, most alder shrubs sampled had either germinated or resprouted, and vegetation productivity inside 60 burn perimeters had recovered to prefire values. Tundra fires resulted in two phases of increased primary productivity as manifested by increased landscape greening. Phase one occurred in most burned areas 3–10 years after fires, and phase two occurred 16–44 years after fire at sites where tundra fires triggered near-surface permafrost thaw resulting in shrub proliferation. A fire-shrub-greening positive feedback is currently operating in the Noatak Valley and this feedback could expand northward as air temperatures, fire frequencies, and permafrost degradation increase. This feedback will not occur at all locations. In the Noatak Valley, the fire-shrub-greening process is relatively limited in tussock tundra communities, where low-severity fires and shallow active layers exclude shrub proliferation. Climate warming and enhanced fire occurrence will likely shift fire-poor landscapes into either the tussock tundra or erect-shrub-tundra ecological attractor states that now dominate the fire-rich Noatak Valley.

Key Points:

- Tundra fires occur preferentially in more productive areas, and tundra vegetation is highly resilient to burning
- Postfire greening occurs in two phases. Phase one occurs in all plant communities immediately after a fire. Phase two occurs where and when postfire shrub expansion is facilitated by permafrost thaw
- The tussock and shrub fire regimes operating in the Noatak may become ecological attractor states elsewhere as tundra fires expand northward

Supporting Information:

Supporting Information may be found in the online version of this article.

Correspondence to:

B. V. Gaglioti,
bengaglioti@gmail.com

Citation:

Gaglioti, B. V., Berner, L. T., Jones, B. M., Orndahl, K. M., Williams, A. P., Andreu-Hayles, L., et al. (2021). Tussocks enduring or shrubs greening: Alternate responses to changing fire regimes in the Noatak River valley, Alaska. *Journal of Geophysical Research: Biogeosciences*, *126*, e2020JG006009. https://doi.org/10.1029/2020JG006009

Received 6 AUG 2020
Accepted 19 DEC 2020

1. Introduction

1.1. The Implications for Changing Tundra Fire Regimes

Wildland fire is an important ecological disturbance in the tundra biome (Rocha et al., 2012), and increased burning will likely accelerate ecosystem responses to ongoing climate warming across certain regions of the biome (Hu et al., 2010; Landhausser & Wein, 1993; Racine et al., 2004). Rapid warming in the Arctic has resulted in permafrost thaw and the expansion of upright shrub communities in many regions (Martin et al., 2017; Smith et al., 2010; Tape et al., 2006), but it may take decades to centuries for landscape responses to be fully realized because ecological responses to changes in climate can take longer in regions like the Arctic where plants are dormant for much of the year (Chapin & Starfield, 1997). In addition, even the Arctic's relatively simple ecosystems have properties that can buffer them from climate warming, with the result that ecological responses can be delayed or muted (Folke et al., 2004; Loranty et al., 2018). The primary negative feedback that currently buffers tundra in the Low Arctic (<70°N) from climate changes is the widespread presence of a surface organic soil horizon (peat), which insulates underlying permafrost from warming air temperatures (Figure 1a) (Baughman et al., 2015; Yi et al., 2007) and resists vegetation changes by virtue of its cold, water-saturated, and acidic growing medium (Tape et al., 2012). But the tundra's peat *can* burn during warm, dry summers (Jones et al., 2009; Mack et al., 2011), and shrub expansion and permafrost thaw can proceed rapidly after fires combust peat (Jones et al., 2013, 2015). In short, when Arctic warming co-occurs with tundra fires, postfire ecosystem responses are more likely to equilibrate with "the new normal" relative to a more tempered response in the absence of fire (Jones et al., 2013; Landhausser &

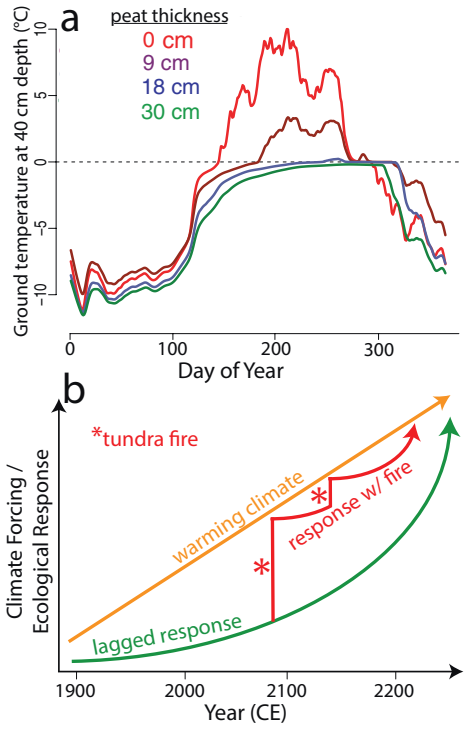

Figure 1. Surface soil organic layers (peat) currently make much of the Low Arctic impervious to change because they buffer underlying permafrost from warming air temperatures and resist shrub expansion. (a) Simulated ground temperature at 40 cm depth during a typical climatic year in Fairbanks, Alaska using the University of Alaska Geophysical Institute's Permafrost Laboratory' permafrost model (Marchenko et al., 2008). Each line represents a simulation with the same climate, but with different peat thickness. (b) Hypothetical climate forcing and ecological responses in the Arctic tundra with and without tundra fires or other disturbances that overwhelm peat's negative feedbacks. The green, "lagged response" curve represents the ecological response in the absence of fires.

Wein, 1993). A summary of how simulated ground temperatures change with varying peat layer thickness and our hypothesized changes of ecological responses to climate forcing with and without fire are shown in Figure 1.

Arctic tundra fires are expected to become more frequent and severe over the next century (French et al., 2015; Hu et al., 2015), and how this altered disturbance regime will affect peat's buffering capacity has global implications. Among the possible impacts of more frequent and severe fires and the associated removal of soil organic horizons is the increased release of soil carbon (C) to the atmosphere as greenhouse gasses during the burning of vegetation and organic soils (Mack et al., 2011; Turetsky et al., 2011) and through subsequent enhanced soil respiration following fire-induced permafrost thaw (Gibson et al., 2018, 2019; Rocha & Shaver, 2011). Although not widely acknowledged in the literature today, at least a portion of this fire-derived carbon release is eventually re-stored in tundra ecosystems during postfire vegetation and soil recovery (Bret-Harte et al., 2013). In this way, some proportion of the greenhouse gas emissions from fires should be considered as a temporary C "loan" to the atmosphere, instead of an irreversible C "gift" to the atmosphere. When considering all aspects of this process, net greenhouse gas effects of tundra fires depend on both the emissions during fires, thaw-driven carbon release, *and* the rates of vegetation productivity and soil recovery following fire. In some cases, postfire nutrient fertilization and permafrost thaw can enhance primary productivity (Barrett et al., 2012; Heim et al., 2019; Jones et al., 2013; Racine et al., 2004; Rocha et al., 2012), while in other cases tundra fires appear to have little effect on long-term primary productivity (Loranty et al., 2014). More observations that describe how vegetation productivity has responded since burning is crucial for determining if, when, and where postfire vegetation trends compensate for C losses during and after fires.

1.2. Postfire Vegetation Responses in Arctic Tundra

In order to understand how tundra fire regimes will change in the future, we first need to understand the limits of the self-maintaining processes that control fire regimes in different parts of the tundra biome. Consider for example the fire regime of tussock tundra vegetation dominated by *Eriophorum vaginatum* L. (cottongrass), whose growth architecture and life history are adapted to optimize growth, reproduction, and longevity on cold, organic-rich soils (Chapin et al., 1979). Individual cottongrass plants often survive low-severity fires because their tillering buds are protected inside a tussock growth form surrounded by years of accumulated dead sedge leaves and tillers (Fetcher & Shaver, 1983; Racine, 1981; Vavrek et al., 1999). Despite being heavily charred during tundra fires, tussocks have the ability to resprout within a year of burning, and then to exhibit enhanced rates of productivity and blooming (Wein & Bliss, 1973; Wein & Shilts, 1976). Racine et al. (1987) pointed out that tundra fires release these fire-adapted cottongrass plants from interspecific competition because: (1) slowly regenerating shrubs growing in inter-tussock areas have the potential to be completely combusted, freeing up light and nutrient resources for the fire-enduring tussocks, and (2) postfire permafrost thaw can lead to enhanced cryoturbation, which exposes mineral soil and is suitable for new tussock colonization with high rates of growth (Hall et al., 1978; Shilts, 1978). Tussock tundra is a relatively flammable vegetation type (Rocha et al., 2012), and low-severity burning releases tussocks from competition and allows them to persist, reproduce, and endure another low-severity fire supported by their nonwoody, fine fuels. Because of these properties, this vegetation-enabled fire regime is widespread in relatively warm areas where tussock tundra routinely dries out enough to carry fires (Racine et al., 1985, 1987).

A much different type of tundra fire regime occurs in areas covered in erect shrub tundra. Once widespread shrub establishment has occurred, fires become more severe than those that burn tussock tundra because greater woody fuels on the landscape are more likely to ignite and carry more severe fires (Higuera et al., 2008; Hu et al., 2015). Increased fire severity is more likely to cause active-layer deepening, which triggers thermokarst activity that in turn promotes the establishment of more shrubs and further increases in primary productivity, including higher rates of woody fuel buildup (Jones et al., 2013, 2015; Lantz et al., 2010, 2013). We call this fire regime feedback the "fire-shrub-greening positive feedback" because the shrub-rich vegetation that proliferates after intense fires supports more severe burning, which then leads to further shrubification, and so on. A variation of this fire regime appears to have maintained a highly flammable, shrub-dominated tundra vegetation in northwest Alaska during the Late Glacial period (14–10,000 years ago) (Higuera et al., 2008, 2009). Areas covered in tussock tundra may be replaced by this alternative, erect-shrub tundra fire regime if sufficient woody-fuel builds-up during the shrub expansion triggered by either future climate warming and/or enhanced permafrost thaw following fires (Lantz et al, 2010, 2013; Myers-Smith et al., 2011).

Despite the existing paradigms applied to tundra fire regimes, several fire-related questions relevant to the future of the tundra biome remain unresolved. These include the extent to which the fire-shrub-greening feedback is currently operating in flammable tundra regions. We also do not know whether ongoing warming will activate this fire-shrub-greening feedback loop in otherwise fire-scarce tundra and usher in a shrubbier vegetation more prone to intense fires. Also unresolved is whether recent warming and enhanced burn severity are able to overcome the self-maintaining features of tussock tundra fire regimes and negative peat feedbacks. This question is important because overcoming these feedbacks would allow the relatively climate-impervious, tussock tundra communities to shift into shrub-dominated communities where the more climate-sensitive, fire-shrub-greening feedback prevails. Here we address these questions by surveying the productivity and types of tundra vegetation that typically burn in tundra fires, and by quantifying how different types of vegetation responded after burning.

1.3. Tundra Fires in Alaska

Currently, tundra fires are most common in warmer, more lightning-rich regions that are covered in shrub and tussock tundra (French et al., 2015; Hu et al., 2015; Masrur et al., 2018; Rocha et al., 2012). Rates of burning dramatically increase where and when mean summer temperatures exceed 11°C, summer precipitation falls below 150 mm (Hu et al., 2015), and summer sea-ice cover is relatively low (Hu et al., 2010). One region where these climatic thresholds are predicted to be crossed in the near future is the North Slope of Alaska, which is the size of Great Britain, and is representative of the broader Low Arctic tundra. Tundra fires are thought to have been rare on the North Slope prior to 1900; however, evidence for large prehistoric tundra fires has recently been discovered there (Jones et al., 2013), and these fires now appear to be occurring more frequently (Chipman et al., 2015; French et al., 2015; Hu et al., 2015).

Because fire has been relatively rare on the North Slope and in other tundra regions with similar climatic regimes, we must look further south for a promising analogue that exhibits how the fire-poor zones of the Arctic *could* be transformed in the warming decades that lie ahead. The fire-rich Noatak watershed is an ideal analogue for the future North Slope because both regions share similar vegetation types and nearly continuous permafrost, which is the literal and figurative foundation of both these region's ecosystems (Jorgenson et al., 2014; Raynolds et al., 2019). In addition, the fire regimes of the Noatak may also serve as a reasonable harbinger for the Arctic foothills region of the North Slope in the future because they share similar topography. Because fire is common in the Noatak, assessing how tundra ecosystems there have responded to recent burning offers a test of the peat-related buffering feedbacks discussed above and provides a case-study for observing the fire-shrub-greening feedback and tussock-fire maintenance cycles. In addition, the Noatak watershed contains latitudinal treeline where the boreal forest transitions into Arctic tundra; two vegetation types potentially in flux due to changes in temperatures and fire regimes.

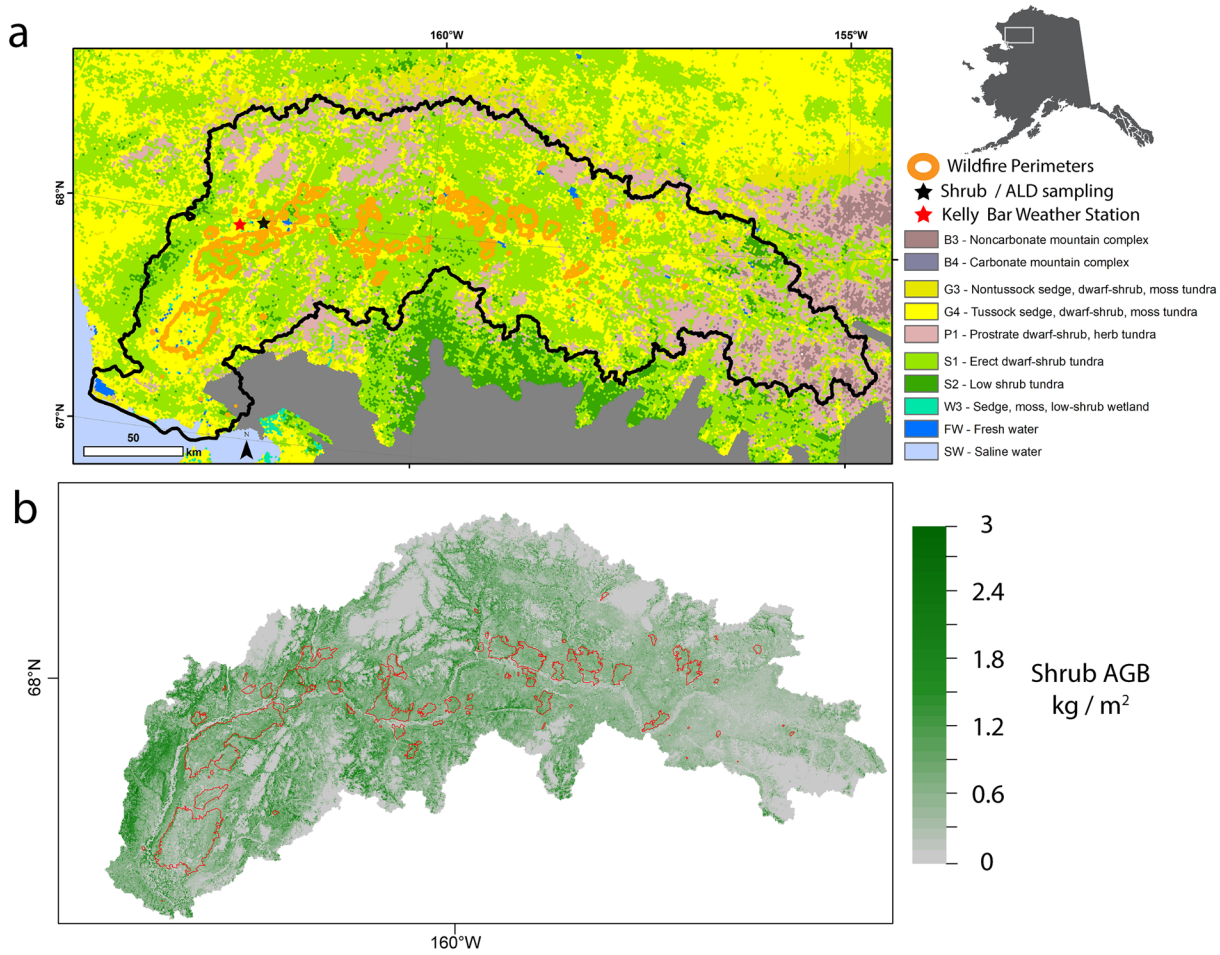

Figure 2. Map of Noatak watershed with shrub sampling site in Northwest Alaska overlain with tundra fire perimeters from the AICC (2019). Base maps include (a) vegetation type (Raynolds et al., 2019) and (b) estimated shrub aboveground biomass (Berner et al., 2018).

1.4. Research Questions

Our overall research question is this: What are the patterns and processes of ecosystem responses to tundra fires in northwestern Alaska? We evaluate this question using shrub dendrochronology, active-layer depth monitoring, and remote sensing. Specific research questions include:

(1) Where on the landscape have tundra fires overcome the negative feedbacks of peat and lead to postfire greening/shrubification?
(2) Is the fire-shrub-greening positive feedback currently operating in the Noatak watershed?

As described above, the implications of these results are relevant to the trajectory of tundra ecosystems in a warmer, more flammable Arctic.

2. Study Area

The Noatak watershed covers 33,000 km^2 and drains the southwestern flank of the Brooks Range in northwestern Alaska. Mean July and January temperatures at the Kelly Bar weather station (N 67.93° W 162.3°; Figure 2) between 1998 and 2019 were 13.8°C and −18.7°C (SD: ±1.7°C and ± 5.1°C), respectively (Horel & Dong, 2010). Annual growing season (May to August) precipitation averages 18.5 cm (SD: 5.6 cm), and snow often covers the ground for 8 months of the year. Boreal forest occurs as gallery forests in the lower reaches of Noatak Valley, and tussock and non-tussock graminoid and erect-, dwarf-, and prostrate-shrub tundra cover the surrounding uplands (Figure 2; Raynolds et al., 2019). The active floodplain surrounding

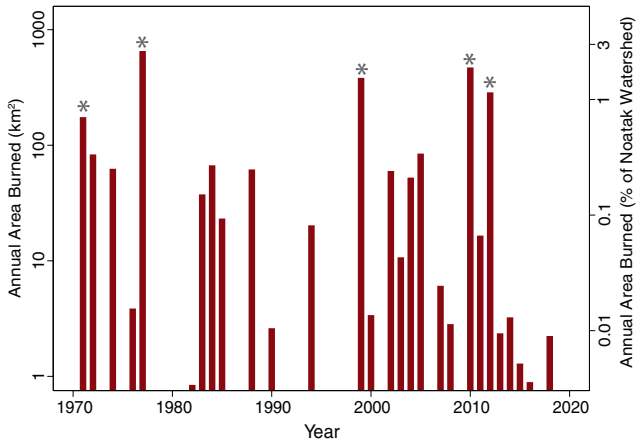

Figure 3. Time series of annual area burned (log scale; left *y*-axis), and percent of watershed burned in the Noatak drainage of Northwest Alaska (log scale; right *y*-axis) (AICC, 2019). Gray stars denote the five years with the most annual area burned between 1971 and 2018.

the lower reaches of the Noatak River is underlain by discontinuous permafrost, while the remainder of the watershed is underlain by continuous permafrost (Jorgenson et al., 2014). The Noatak watershed has a complex glacial history with multiple late-Quaternary ice advances from the Brooks Range leaving diverse glacial till, drift and lake deposits, which in some places are overlain or reworked by Holocene fluvial terraces, alluvial fans, and colluvium (Hamilton, 2009).

Tundra fires occur regularly in the Noatak watershed, typically below 600 m a.s.l. (Racine et al., 1985). On average, 0.2% of the watershed has burned annually since reliable record-keeping began in 1970 (Figure 3), which is equivalent to a 476-year fire rotation period (length of time required for entire area of the watershed to burn). Paleo-fire records based on lake-sediment charcoal indicate that fire return intervals (years between fires at a given location) in the Noatak Valley have been 100–285 years in the past two millennia (Chipman et al., 2015; Higuera et al., 2011). In historical times, most burning occurred during five relatively warm summers (noted by gray stars in Figure 3) (1972, 1977, 1999, 2010, and 2012) (AICC, 2019). Fires in the Noatak are typically *not* ignited in areas covered in boreal forest; instead, most fires are ignited by lightning strikes in upland communities of tussock and shrub tundra. Forest edges and stringers of boreal trees often act as fire breaks (Racine et al., 1985). Most of the Noatak watershed is designated as a National Park Service Federal Wilderness, and humans have had few impacts on its fire regime (Racine et al., 1985).

3. Methodological Background

Because most fires in the remote Noatak region have not been directly monitored in real time, we employ methods that retrospectively describe the ecological impacts of fires. These methods include dendrochronology, which can estimate the rate of shrub growth and shrub recruitment at three adjacent sites possessing different burn histories and postfire permafrost responses. Dendrochronology measures the radial growth of woody plants, and tundra shrub-ring analysis has proven a reliable surrogate for annual primary productivity for both shrubs and their nonwoody counterparts in Arctic Alaska (Andreu-Hayles et al., 2020; Berner et al., 2020).

We also use the Landsat satellite record of remotely sensed vegetation productivity to describe postfire vegetation responses from 1989 to 2016. For this analysis, we use a chronosequence of different aged burns. The 2-band enhanced vegetation index (hereafter, EVI2; Jiang et al., 2008) was used as a proxy for annual photosynthetic activity in all available years at randomly sampled points that differ in burn history and other biophysical characteristics (see below). The EVI2 represents a snapshot of the degree of red absorption and therefore of landscape greenness after taking into account atmospheric absorption and surface reflectiveness. We chose EVI2 over the normalized differential vegetation index (NDVI) because EVI2 is more sensitive to the postfire responses of tundra vegetation and more accurate in quantifying changes in tundra vegetation canopy structure (Rocha & Shaver, 2009), which is a common vegetation response to wildfires in the Noatak watershed (Racine et al., 2006). EVI2 is linearly related to both tundra net ecosystem exchange (Rocha & Shaver, 2011) and leaf area index (Rocha & Shaver, 2009), as well as correlated with gross primary productivity across ecosystem types (Rahman et al., 2005).

In order to quantify how well EVI2 captures the impact of tundra fires on vegetation, we compared each annual, burned EVI2-value to the entire unburned EVI2 distribution for that same year (hereafter, $EVI2_b$). This $EVI2_b$ index thereby captures the greenness of burned vegetation *relative* to unburned vegetation during the same growing season (Figure 4b). Without this relative perspective, postfire vegetation changes due to the effects of burning cannot be separated from ongoing, nonfire-related greening or browning trends experienced by vegetation throughout this region of the Arctic (Figure 4a). This is particularly important in tundra regions, where significant warming-driven greening trends have occurred in the last several decades

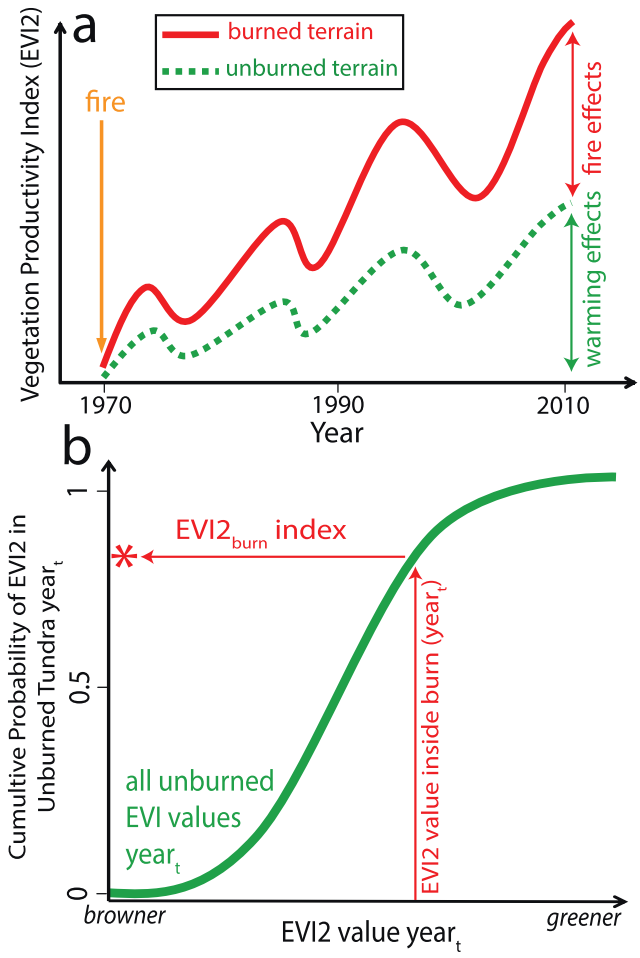

Figure 4. (a) Remotely sensed vegetation indices are affected by both climate and by fires in the Arctic tundra. (b) In order to isolate the effects of fires, we calculated the $EVI2_{burn}$ index by placing each annual EVI2 value in burned areas into the context of all unburned observations for the same calendar year.

(Berner et al., 2020; Myers-Smith et al., 2020). By using the $EVI2_b$ index, we remove these climate-driven greening trends to isolate the effects of tundra wildfire on vegetation productivity.

4. Methods and Analysis

4.1. Field Collections, Dendrochronology, Data Analysis

While visiting burn scars in the area affected by both the Avan Fire (1972; 19.7 km^2) and WTK-N-60 Fire (1984; 18.1 km^2) in late August 2017, we measured active-layer depths (ALD; maximum late-summer thaw depth) using a tile probe and also sampled the annual rings of shrub ramets. At three locations with different burn histories, ALD measurements were made 2–3 m apart along 2–3 100-m-long transects. Three sites were sampled: (1) burned by WTK-N-60 fire (burned once) (N 67.982804° W 161.978916°), (2) burned by both the Avan and the WTK-N-60 fires (burned twice) (N 67.986404° W 161.973789°), and (3) a nearby area outside both fire perimeters (unburned in historical times) (N 67.991609° W 162.003299°). Although the once-burned sampling site does not fall within the mapped fire perimeter of the WTK-N-60 Fire (AICC, 2019), there was significant field evidence of shrubs burning in 1984, but not in 1972.

At each site, 22 to 29 cross-sections of *Alnus viridis* (green alder; hereafter, alder) ramets were collected with a hand saw at their root collar. We sampled one of the largest ramets in each clone. Cross-sections were sanded with increasingly fine sandpaper up to 600-grit to reveal ring boundaries. Ring widths were measured digitally to the nearest 0.001 mm in high-resolution scans using the computer program CooRecorder 8.1. Ring-width series were visually and statistically cross-dated using standard dendrochronological techniques (Holmes, 1983; Stokes, 1996) to ensure that each ring was assigned the correct calendar year. The calendar year of the pith serves as a limiting age estimate for shrub establishment because the individual could be older if there were older, unsampled ramets. Ring widths were used to calculate the Basal Area Increments (BAI) for each ramet (Biondi, 1999), which represents the area of wood (mm^2) grown by the stem each year. We use BAI as a proxy for annual productivity of shrub populations exposed to differing burn histories.

We compared ALDs and shrub BAI at sites with different burn histories using a two-tailed Student's *t*-test. In the case of shrub BAI, a *t*-test comparison for the combined growth indices of all ramets from each site for each calendar year was used to determine when shrub populations with different burn histories had significantly different mean growth rates.

4.2. Remotely Sensed Data

4.2.1. Baseline Maps

We used the Alaska Interagency Coordination Center's (AICC) burn-perimeter database managed by the Bureau of Land Management as a record of fire history and fire extent in the Noatak River watershed (Figure 2) (AICC, 2019). To observe how different landscape types responded to fires of varying severity, the AICC perimeter data were combined with a variety of environmental maps (Figure 2) including permafrost type ("discontinuous" or "continuous"), segregated ice content (<50% or >50%) (Jorgenson et al., 2014), vegetation type based on the Circumpolar Arctic Vegetation Map (CAVM; Raynolds et al., 2019), surficial geologic unit (Hamilton, 2010), shrub aboveground biomass (shrub AGB; Berner et al., 2018), and burn severity (for portions of fires occurring after 2001; Loboda et al., 2018).

4.2.2. Vegetation Flammability Index (FI)

We calculated a FI for seven different CAVM vegetation types (Raynolds et al., 2019), including: fellfield barrens, erect shrub tundra, low shrub tundra, non-tussock sedge tundra, prostrate shrub tundra, wet sedge tundra, and tussock sedge tundra.

$$\mathrm{FI} = V_b \,/\, V_t \tag{1}$$

where V_b is the vegetation type's percent cover within historically burned areas in the Noatak River watershed, and V_t is the percent of the total watershed occupied by that same vegetation type. A FI index >1 indicates that a vegetation type is over-represented in areas that burned and is therefore relatively fire prone.

4.2.3. Quantifying Vegetation Productivity

We generated ~7,200 random sampling points in the Noatak River watershed that varied in burn history and fire severity, as well as in permafrost, surficial geology, and vegetation type. Nonvegetated areas (including rocks, water, gravel bars), and areas with high tree cover, *sensu* Hansen et al. (2013), were excluded when generating the random points. These random points included 3,137 points that went unburned during the historical record, and 4,066 points that were burned by one of 60 different fires between 1971 and 2016. Each sample point was at least 250 m away from a burn perimeter and at least 250 m away from any other sample point. A >250-m burn perimeter buffer was used because we found that the AICC fire perimeters were sometimes off by up to 250 m when compared to the fire boundaries based on post-burn satellite imagery. The number of sampling points within each burn was proportional to fire size; we populated each fire scar with sampling points until the 250-m inter-point distance-criteria could no longer be met. A series of unburned sampling points were randomly selected for each fire within a donut-shaped polygon surrounding each fire whose inner margin was >250 m outside the fire perimeter. The dimensions of these unburned polygons varied according to the size of each burned area. The number of unburned points for each fire roughly corresponded to the number of points within the nearby burn, and some unburned points serve as unburned controls for more than one overlapping fire. Each point was then assigned properties describing permafrost type, vegetation type, surficial geology, and burn severity based on the maps referred to above. Remotely sensed vegetation indices measured at these sampling locations were used to characterize the vegetation that burned and how that vegetation responded in the years following a fire.

We generated peak summer EVI2 time series for each sampling point using surface reflectance measurements from Landsat 5 (TM), 7 (ETM+), and 8 (OLI) (Masek et al., 2006; Vermote et al., 2016), which we downloaded and processed using Google Earth Engine (Gorelick et al., 2017). Following the approach of Berner et al. (2020), we quality-screened the measurements and then cross-calibrated EVI2 among Landsat sensors using a machine learning approach. We estimated annual peak summer EVI2 for each sampling point as the median of observations during the period when the watershed wide mean EVI2 was within 90% of the max (Julian days 182–227).

4.2.4. A New Index for Assessing Postfire Vegetation Change in Arctic Regions

We calculated an EVI2 burn index ($\mathrm{EVI2_b}$) for each available year at every sampling location by transforming each annual burned observation (burned: $\mathrm{location}_x$, year_t) into a percentile of the cumulative probability distribution of all unburned EVI2 observations from that same calendar year (unburned: $\mathrm{location}_{\mathrm{all}}$, year_t) (Figure 4b). In order to quantify postfire greening trends in different types of permafrost, vegetation, and geologic units, we transformed each annual burned EVI2 of a given landscape type (burned: $\mathrm{location}_x$, year_t, $\mathrm{landscape}_q$) into a percentile of the cumulative probability distribution of the annual unburned EVI2 observations located in that same landscape type during the same calendar year (unburned: $\mathrm{location}_{\mathrm{all}}$, year_t, $\mathrm{landscape}_q$). As an example, $\mathrm{EVI2_b}$ values of 0.5 correspond to the median of unburned values for that same year. Continuing with this example, $\mathrm{EVI2_b}$ values of <0.5 are on the lower productivity side ("brown side") of the unburned spectrum, and values >0.5 are on the greener side of the unburned spectrum for the corresponding year.

4.2.5. Quantifying Postfire Vegetation Change

To determine whether burning led to an increase in shrub cover, we mapped shrub aboveground biomass (AGB; kg $\mathrm{m^{-2}}$) at 30-m resolution across the Noatak Valley and then compared shrub AGB in burned and

unburned areas. We mapped shrub AGB using a regional Landsat 8 NDVI composite mosaic (2015–2019) and a statistical relationship between shrub AGB and Landsat NDVI that was developed using biomass harvests at field sites across northwestern North America (Berner et al., 2018). Landsat NDVI explained 82 (59, 88)% of the spatial variability in shrub AGB across field sites with a root mean squared error (RMSE) of 0.24 (0.17, 0.48) kg m^{-2} (95% Monte Carlo confidence intervals; Berner et al., 2018). Multiple sources of uncertainty affected the AGB – NDVI relationship, including Landsat sensor calibration and sampling error within each field site. We acknowledge pixel-level uncertainty associated with the shrub AGB estimates but did not have adequate field data to evaluate the accuracy of the shrub AGB map in the Noatak region. However, the same approach was recently used to map shrub AGB across the neighboring North Slope, where modeled shrub AGB tracked field measurements of shrub height ($r_s = 0.88$), remote-sensing derived shrub canopy cover ($r_s = 0.76$), and spatial patterns of shrub AGB evident in high-resolution satellite imagery (Berner et al., 2018).

After mapping shrub AGB, we then created another randomly sampled set of data-points with greater sampling density per fire (in this case 21,580 total points: 11,939 burned points, and 9,641 unburned points). Only fires with >25 sampling locations for burned and unburned situations were compared ($n = 35$ fires). Each point was assigned the mean shrub AGB within a radius of 25 m around the data point. Because these shrub biomass estimates used satellite imagery collected between 2015 and 2019, we excluded fires that occurred after 2012 so we could focus on vegetation change occurring after the initial postfire recovery period of three years (see Results for our estimate of the duration of this postfire recovery period). Focusing on older fires also reduced the possibility of overestimating shrub AGB in recently burned areas due to charred surface soils artificially increasing NDVI (*sensu* Rocha & Shaver, 2009). All shrub AGB estimates in burned and unburned areas were standardized relative to each other for each fire, and we then compared the estimated shrub AGB at all burned sampling points relative to that of unburned sampling points using a Kolmogorov-Smirnov (K-S) test. We acknowledge that there are intra-pixel uncertainties associated with the shrub AGB estimates, however we focus on the mean predicted estimates for this statistical test.

To quantify fire-induced vegetation change, we organized all $EVI2_b$ values by year-since-last-fire. For example, the 1999 $EVI2_b$ value for a point located in an area that burned in 1984 (15 years-since-fire) was binned with a 2015 $EVI2_b$ value from a sample point that burned in 2000 (also 15 years-since-fire). We excluded year-since-fire values that had less than 10 fires contributing to the annual time-since-fire bin. After removing those values with <10 fires contributing, we analyzed the $EVI2_b$ time series from 10 years before fires to 44 years after fires (55 years total). All $EVI2_b$ observations for each location for each available year were combined to obtain the mean and 95% confidence interval for each year-since-fire. We do not take into account instrument-related errors in our analysis.

A *prefire* $EVI2_b$ baseline consisted of all values occurring between 5 and 1 year *before* fires ($EVI2_{b\ preburn}$). This 5-year window of $EVI2_{b\ preburn}$ (5–1 year before fires) was compared with succeeding 5-year windows of $EVI2_{b\ postburn}$ values (0–5, 1–6, 2–7,... years-since-fire) using Student's *t*-tests. One-sided tests were used for these pre and postfire comparisons because we hypothesized that, after an initial postfire recovery period, vegetation indices would show postfire greening trends. We quantified postfire browning or greening patterns by taking the mean difference between various $EVI2_{postburn}$ values (annual and five-year windows) and the mean of all $EVI2_{preburn}$ values. We also calculated the percent of $EVI2_{b\ postburn}$ change relative to the $EVI2_{b\ preburn}$ value. These analyses were repeated for $EVI2_b$ values in discreet vegetation, permafrost, geologic, and burn severity types described above. For this landscape-specific postfire greening analysis, we only considered year-since-fire $EVI2_b$ observations that had at least three different fires contributing to the data set in each landscape type.

To determine how postfire vegetation recovery and greening compensated for the loss of productivity during and immediately following burns, we first estimated what $EVI2_b$ would be like during the 44-year postfire period in the absence of fire, using 10,000 time-series of randomly generated postfire $EVI2_b$ data sets based on the mean and variability of prefire $EVI2_b$ observed in the 10 years before fires. We then calculated the mean and 95% percentage of $EVI2_b$ loss and gain of the observed postfire data relative to the data sets that simulated what EVI2b would be like without a fire between 0 and 44 years after fire. Cumulative postfire greening compensated for $EVI2_b$ loss during fire when these cumulative percentages became >100%.

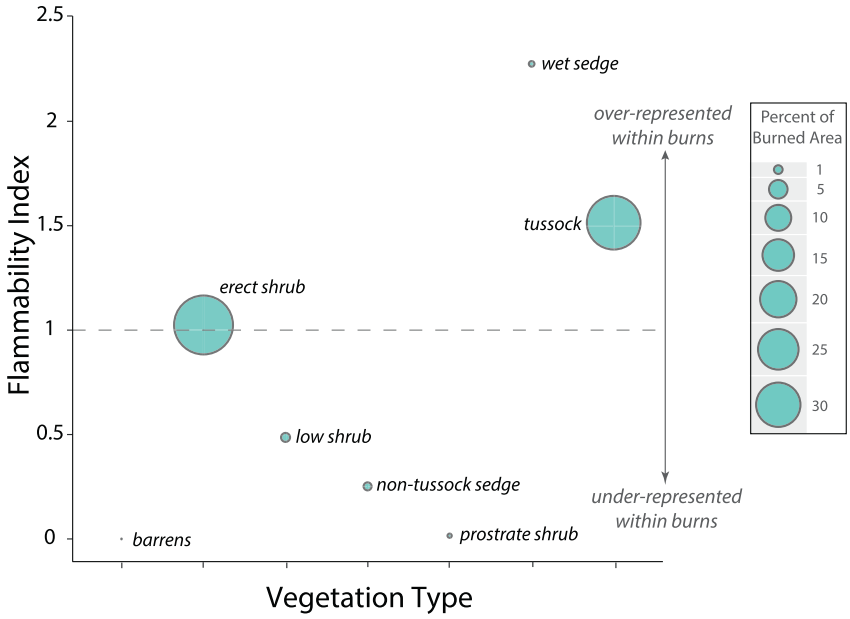

Figure 5. Flammability index and percent of total burned area (AICC, 2019) for the seven different vegetation types in the Noatak watershed (Raynolds et al., 2019).

5. Results

5.1. Fuel Type and Postfire Vegetation Recovery

Fuel type strongly affected the distribution of fires in the Noatak River valley. Areas of erect-shrub tundra and tussock tundra had relatively high flammability indices (1.1 and 1.5) and made up the majority of total area burned from 1972 to 2016 (53.4% and 44.1%, respectively, and a total of 97.5% of all burn area; see Figure 5 and Table 1). Wet sedge tundra had the highest FI (2.3) but only made up 0.38% of the total burned area. Areas mapped as prostrate-shrub tundra, barrens, non-tussock sedge tundra, and low shrub tundra had relatively low flammability indices (0.02, 0.00, 0.20, and 0.49, respectively) and made up a small amount of total burn area (0.2%, 0.0%, 0.8%, and 1.1%, respectively).

Within-burn $EVI2_b$ and raw EVI2 values collected prior to fires are also indicative of what types of vegetation tend to burn in the Noatak. During the 5 years before burning, tundra vegetation inside burn perimeters was significantly more productive than the median EVI2 of areas that went unburned ($EVI2_b > 0.5$), and EVI2 values were significantly greater inside than outside burn perimeters (Figures 6a and S1; prefire $EVI2_b$ index (mean, SD): 0.6 ± 0.18). Areas that burned more severely had a higher $EVI2_b$ index before burning (Figure S2) (low severity (mean, SD): 0.51 ± 0.18, medium-low severity: 0.63 ± 0.16, medium-high severity: 0.68 ± 0.19, high severity: 0.70 ± 0.16). Overall, tundra fires were more likely to occur in vegetation types with higher AGB, and the areas that burned more severely had higher prefire $EVI2_b$ productivity indices.

Table 1
Flammability Indices of Vegetation Types in the Noatak Watershed (Raynolds et al., 2019)

Vegetation type	Percent of watershed	Percent of burn area	Flammability index
Barrens	0.1	0	0
Non-tussock	3.3	0.8	0.3
Tussock	29.1	44.1	1.5
Prostrate shrub	12.9	0.2	0.0
Erect shrub	52.1	53.4	1.0
Low shrub	2.2	1.1	0.5
Wet sedge	0.2	0.4	2.3

$EVI2_b$ was reduced (from $EVI2_b$ mean, SD: 0.61 ± 0.18) by an average of 77% (0.14 ± 0.17) during the summer when the fire occurred, and by 62% (0.23 ± 0.16) and 24% (0.46 ± 0.17) during the first and second summer following fires, respectively (Figure 6a). Mean $EVI2_b$ became higher than prefire values during the third summer after a burn. As burn severity increased, immediate postfire $EVI2_b$ values decreased, and the postfire recovery period took longer (Figures 7 and S2). For example, $EVI2_b$ in areas that burned in high severity fires (low severity fires) were reduced

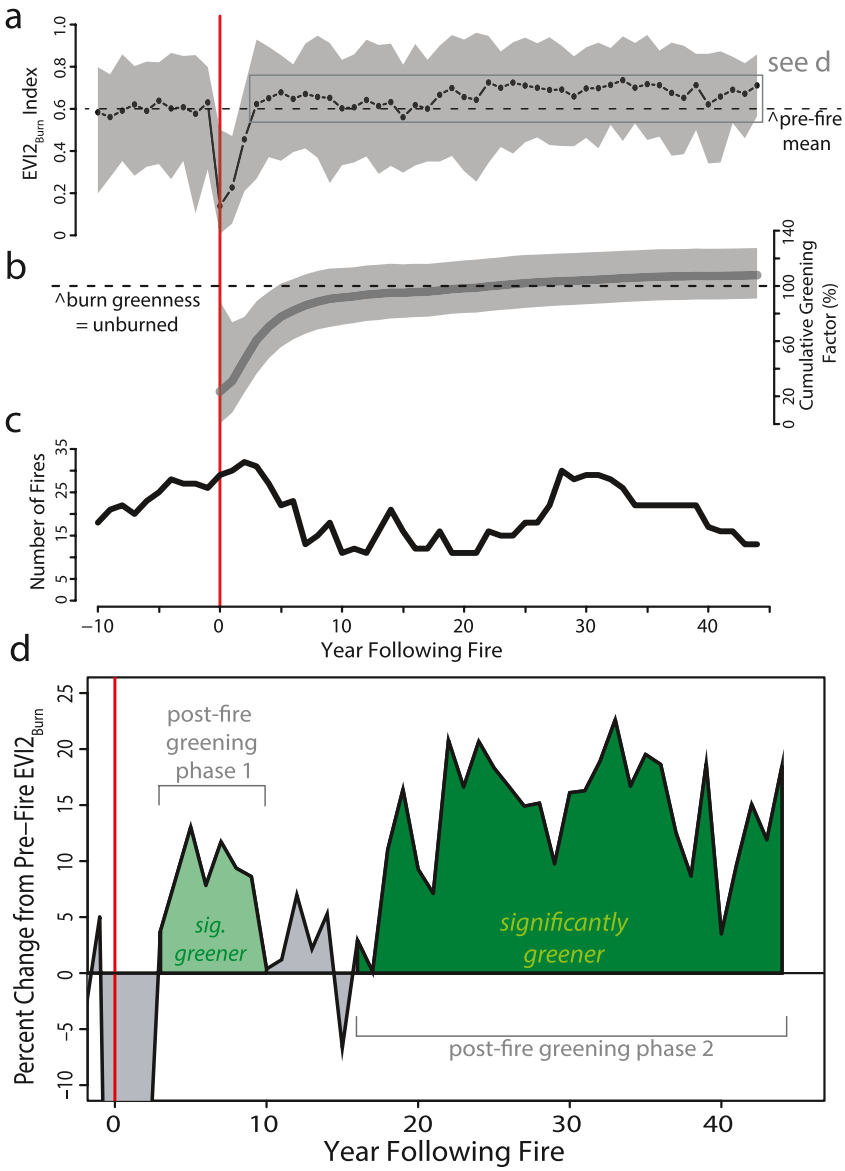

Figure 6. (a) Mean and 95% confidence intervals of $EVI2_b$ indices for all fires. Dashed line is the 10-year prefire mean (0.60). (b) Cumulative postfire greening relative to preburn $EVI2_b$ values. Percentages >100 indicates postfire greening has compensated for $EVI2_b$ reduction during the three years following burning. (c) Number of fires with $EVI2_b$ values contributing to this record over time. Vertical red line indicates the year of fire event. (d) Closeup of (a) showing the percentage change of $EVI2_b$ relative to prefire values (5–1 year before fires). Green shading indicates when postfire $EVI2_b$ values are significantly greater than those 5–1 years before fires ($p < 0.05$).

by 73%, 94%, and 61% (74%, 34%, 9%) during zero, one, and two years after fire, respectively, and did not recover to prefire values until 5 (3) years after fires (Figure 7).

Field observations and shrub dendrochronology from the Avan – WTK-N-60 burn-overlap sites indicate that vegetation began regenerating a year or two after burning in 1984, or, in some cases, plants survived the fire with only minimal damage. Supporting observations include: (1) 45% of the sampled alder stems germinated within three years of the 1984 fire (Figure S3), (2) Five alders survived the 1984 fire with only minor stem damage represented by a dark burn scar in the ring that was grown in the summer of 1984 (Figure S4), and (3) Living cottongrass tussocks had charred outer leaf shoots, indicating at least some of them survived the burn. Collectively, the field observations, dendrochronology, and remotely sensed data suggest that, with

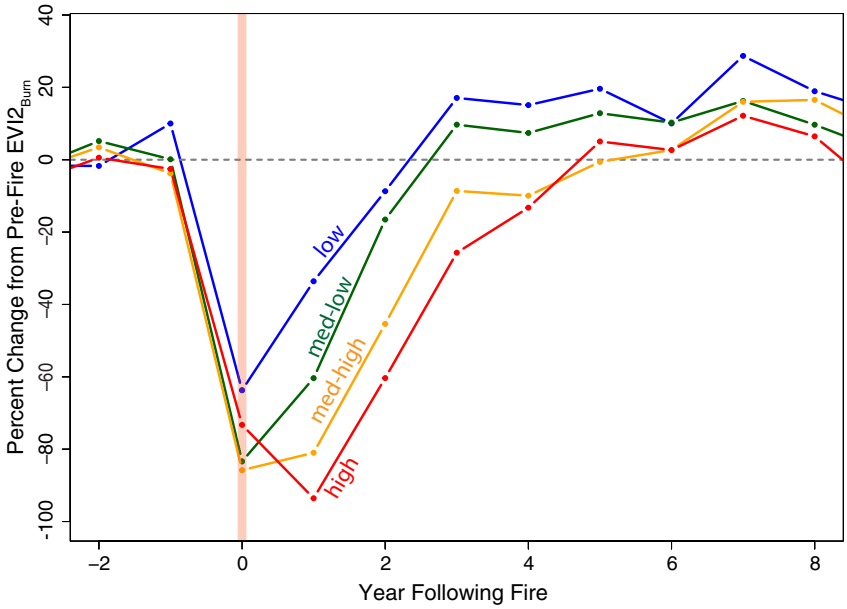

Figure 7. Percentage change of postfire $EVI2_b$ relative to the 5 year before fires for locations that varied by burn severity. Burn severity classification is from Loboda et al. (2018).

the exception of the most severely burned areas, tundra vegetation typically returns to prefire greenness within just three years following a low-to-moderate severity fire.

5.2. Postfire Greening and Permafrost Thaw

Following the initial postfire recovery period, burned areas showed higher primary productivity than before fires in the burned area as well as those recorded in adjacent unburned areas during corresponding years. Between 3-10 years and 16–44 years following a fire, the $EVI2_b$ index was 8% and 14% higher on average than prefire values, respectively (Figure 6d). In addition, mean shrub AGB for 2015-2019 was significantly higher inside 26 of 35 burn perimeters ($p < 0.05$) (Figure S5). When shrub AGB estimates for all pre-2012 fires combined, we found that burned areas had 3.35% higher shrub AGB than in nearby unburned terrain (mean burned AGB: 0.635 kg m^{-2}; mean unburned 0.615 kg m^{-2}; $p < 0.05$; Figure S6).

On average, fires began having a cumulative, net greening effect on tundra vegetation ~20 years after burning (Figure 6b). Around 40 years after burning, fires caused cumulative $EVI2_b$ to be 7% greener than what it would have been without fire (Figure 6b). If postfire $EVI2_b$ maintained the same mean for the next 15 years (55 years after fires), burned vegetation would be outside the upper 95% confidence interval of what they would have been without fire.

At the Avan – WTK-N-60 overlap site, active layer depths were 30% greater in twice-burned areas (ALD: 54.2 ± 13.3 cm) than those that remained unburned since 1970 (ALD: 40 ± 8.6 cm), and radial growth rates of shrubs were 2–3X greater in twice-burned areas than their unburned counterparts. In areas that burned only once (ALD: 44.3 ± 7.2), active layer depths were 10% deeper than in unburned areas, while radial growth rates of shrubs were not significantly different from those growing in unburned areas (Figures 8 and S7). After a period of slow growth, it took between 5 and 13 years after the 1984 fire for annual radial growth rates in shrubs growing in twice-burned terrain to exceed those in shrubs growing in terrain that burned once or that went unburned (Figure 8 and S7). Qualitative field observations indicated that the largest, fastest-growing shrubs were found growing in areas with the deepest, postfire active layers. Dendrochronology cross-dating statistics can be found in Table 2 and BAI results are depicted in Figures 8 and S7.

Postfire greening was more pronounced at sampling points with these characteristics: (1) burned at low to medium severity (Figure S2), (2) were underlain by continuous permafrost (Figures 9a and S8), (3) were covered in erect shrub tundra (Figures 9b and S9), (4) were underlain by >50% segregated ice (Figures 9c

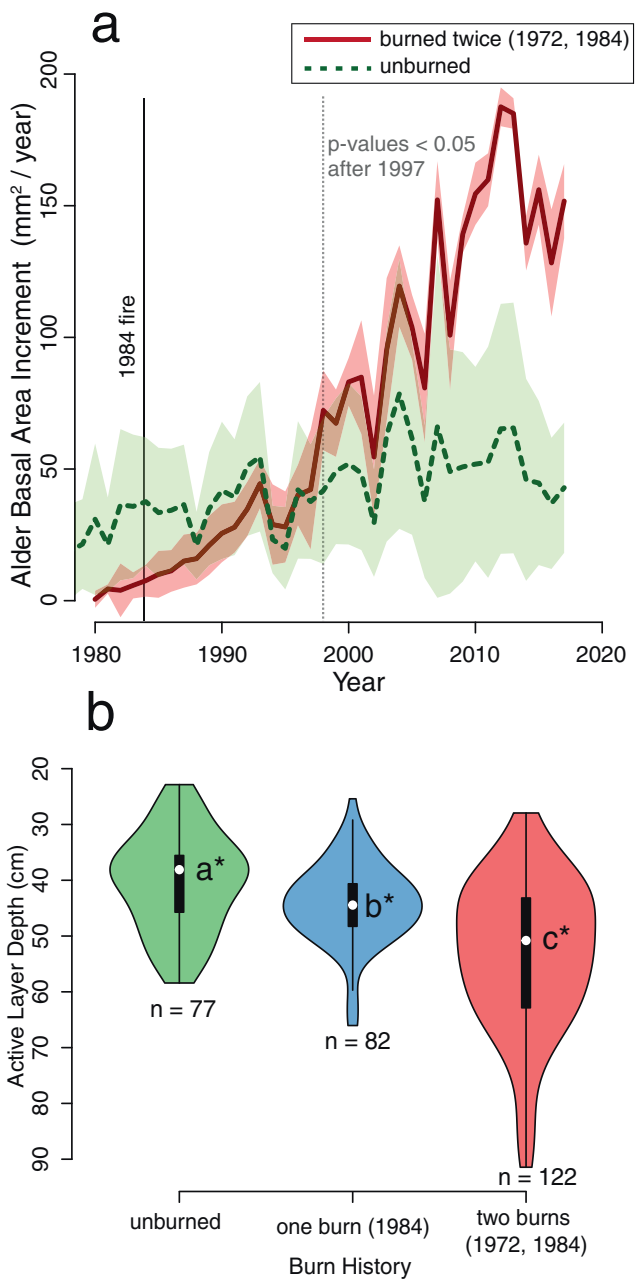

Figure 8. (a) Means (lines) and standard-deviation ranges (shading) of basal area increments of alders growing in areas experiencing different burn histories. Years to the right of dotted lines indicate times when alders growing in an area that burned twice (1972 and 1984) had significantly greater growth rates than alders growing in an area that went unburned since at least 1970, (b) Active layer depths in areas with different burn histories showing the median (dots), interquartile range (vertical black bars), 1.5x interquartile range (vertical black lines) and the kernel density estimation to show the probability distribution of the data (outer margin). Different letters denote significantly different means ($p < 0.05$).

and S10), and (5) were located in coarse-grained, steeper landscape unit types more likely to erode (Figure S11). In areas that experienced low-severity fires, the greening that occurred 3–16 years postfire was 17% higher than prefire values (Figures S2). In contrast, the postfire greening for medium-low-severity and medium-high-severity fires only occurred between 5–7 years following fires and 9–10 years following fires, respectively (Figure S2). Burned areas underlain by discontinuous permafrost (portions of 18 out of 60 fires) did not exhibit postfire greening, and burned areas underlain by continuous permafrost (54 of 60 fires) exhibited a two-phase greening pattern between 3 and 14-years (14%) greener than prefire vegetation and between 18 and 38-years following fires (18% greener than prefire vegetation) (Figures 9a and S8). Postfire greening was more pronounced, persistent, and prolonged in areas of erect shrublands than in non-tussock graminoid tundra (Figures 9b and S9). Burned tussock tundra experienced only sporadic postfire greening episodes (Figures 9b and S9). Land unit types underlain by coarser-grained sediments (glacier drift, and colluvium, alluvium, and alluvial fans) had higher postfire greening trends than those with finer surface sediments (glacial lake deposits and stream terraces) (Figure S11).

In summary, fires are more likely to burn in areas with higher fuel loads, and, after a 3-year recovery period, the occurrence of a fire results in more productive vegetation, which, in many cases, involves shrub proliferation and/or expansion. Postfire greening is more pronounced after low-severity fires that occurred in shrubby areas underlain by continuous permafrost and coarse-grained sediment (Figure 10). The beginning of the second phase of postfire greening observed in $EVI2_b$ (16-years following fires) roughly coincides with the time it takes for shrubs growing on twice-burned landscapes to exceed the growth rates of shrubs growing in nearby areas that either burned once or went unburned (Figures 6d and 8).

6. Discussion

6.1. The Nature of Tundra Fire Fuels in the Noatak

Vegetation types dominated by erect shrubs and cottongrass tussocks comprise most of the area burned (97%) in the Noatak watershed and are over-represented in burned areas relative to the total area they occupy in the Noatak watershed (Figure 5). A high FI for erect shrub tundra (>1), along with a >0.5 $EVI2_b$ during the 10 years preceding fires (Figure 6a), indicate that areas with greater primary productivity are more flammable. In addition, a higher prefire $EVI2_b$ in more severely burned areas indicates that the most productive landscapes carried fires that combusted a greater portion of the vegetation and soil-surface organic horizons, which resulted in a longer postfire vegetation recovery times (Figure 7). In addition, the areas of tussock tundra that burned were relatively productive before burning compared with unburned tussock tundra (mean prefire EVI2b: 0.69 ± 0.18; Figure S9), implying that fuel limitations on fire spread may operate in graminoid tundra as well. Overall, these data suggest that the amount and type of fuels influence the distribution and severity of tundra fires in this relatively flammable area of the Arctic, and that most tundra burning occurs in just two vegetation types (tussock and erect shrub tundra). The vegetation-mediated fire regimes that exist in the Noatak imply that a warming-driven increase in tundra fire occurrence will be moderated by the velocity and pathways of

Table 2
Dendrochronology Statistics of All Alder Shrubs Sampled Within and Near the Avan and WTK-N-60 Fires

Start year	End year	Number of radii measured	Number of between-radii correlations	Rbar between cores	Expressed population signal (EPS)	Signal to noise ratio
1948	1967	21	55	0.15	0.73	2.63
1958	1977	32	120	0.25	0.88	7.09
1968	1987	93	210	0.16	0.89	7.92
1978	1997	124	595	0.30	0.97	36.61
1988	2007	142	4,753	0.33	0.98	61.99
1998	2017	142	3,570	0.35	0.99	70.33
All		142	3,936	0.28	0.96	23.99

warming-driven vegetation change (as in Higuera et al., 2009). In other words, only when plant communities change, will their fire regimes follow.

6.2. Postfire Vegetation Recovery

The circa three-year postfire vegetation recovery that we see here has been observed in other tundra regions of Alaska (Rocha et al., 2012). This is a rapid recovery compared with the boreal forest, where more severe, ground-carried crown fires and multiple seres of plant succession involve slow-growing conifers. The shorter postfire recovery time observed in the Noatak can also be attributed in part to tundra fires being lower in severity than forest fires because of significantly lower fuel loads, and because of the thermal state of the soil when tundra fires occur. Regarding the latter, most wildland fires in in the Noatak Valley occur before July 5 (AICC, 2019), when active layers are still thin and both plant rhizomes and seed banks are sheltered from burning by wet or frozen soils (Hinzman et al., 1991), enabling them to resprout soon after fire occurrence.

As observed in other remote-sensing and field-based studies, the rapid recovery of land-surface greenness following tundra fires suggests that the initial stage of postfire vegetation succession involves resprouting of plants that survived the fire (Bret-Harte et al., 2013; Landhausser & Wein, 1993; Racine et al., 1987; Wein & Bliss, 1973). We observed tundra fires partially scarred the cambium of living shrubs that survived the fires, and thus allowing faster replenishment of woody fuels in postfire tundra (Figure S4). It remains to be seen how common fire-scarring is among tundra shrubs, and what life history traits tundra shrubs have evolved for fire avoidance. The resistance of shrub ramets to fire damage has implications for the speed of postfire vegetation recovery, and for dating prehistoric fires using wood morphology (i.e., Gaglioti et al., 2016). Other life-history traits of the dominant plants that serve as fuel for tundra fires include the protected rhizomes of fire survivors like cottongrass and hydrophillous and mesic sedges, which, shortly after a fire, are able to resprout from unburned tiller buds (Fetcher & Shaver, 1983; Racine et al., 1987; Vavrek et al., 1999; Wein & Bliss, 1973).

The rapid recovery of graminoid tundra is probably also enabled by enhanced plant growth of fire-survivor species following release from competition with plants that do not readily survive burns. As Racine et al. (1987, 2004) pointed out, above-ground biomass of dwarf shrubs in inter-tussock areas are often consumed by fire, and their demise temporarily enhances the growth of the fire-enduring cottongrass tussocks. In better-drained shrub-tundra areas, fires can also trigger the germination of *Calamagrostis canadensis* grass (bluejoint grass), which flourish once the shrubs are killed by burning (Jandt et al., 2012; Jones et al., 2013; Tsuyuzaki et al., 2018; Wein & Bliss, 1973). Overall, a shallow active layer during burning, postfire resprouting, and removal of shrub competitors allow $EVI2_b$ values in the Noatak to recover their prefire values within three years in all but the most severely burned areas (Figure 7). Longer (>3-year) postfire recovery also occurs in areas where dominant prefire vegetation was located on floodplains (Figure S11). At such sites, it can take several years for tall-shrub and tree canopy structure to re-form (as in Johnstone & Chapin, 2006).

6.3. A Two-Phase Postfire Greening Pattern

The distribution and timing of the first postfire greening phase provides clues about the processes that cause postfire vegetation to become greener than before fires between three and ten years following a burn. This first greening phase is observed in the $EVI2_b$ values when all data points are combined (Figure 6d), at sites that burned with low severity (Figure S2), as well as sites underlain by continuous permafrost (Figure 9a), have >50% segregation ice (Figure 9c), located on steeper terrain underlain by coarser lithologies (Figure S11), and vegetated by erect shrub tundra (Figure 9b). Earlier work indicates that plant and soil combustion during boreal and tundra fires tends to enhance nutrient availability in the years following fire, including available phosphorous and nitrogen, which typically limit primary productivity in the Low Arctic

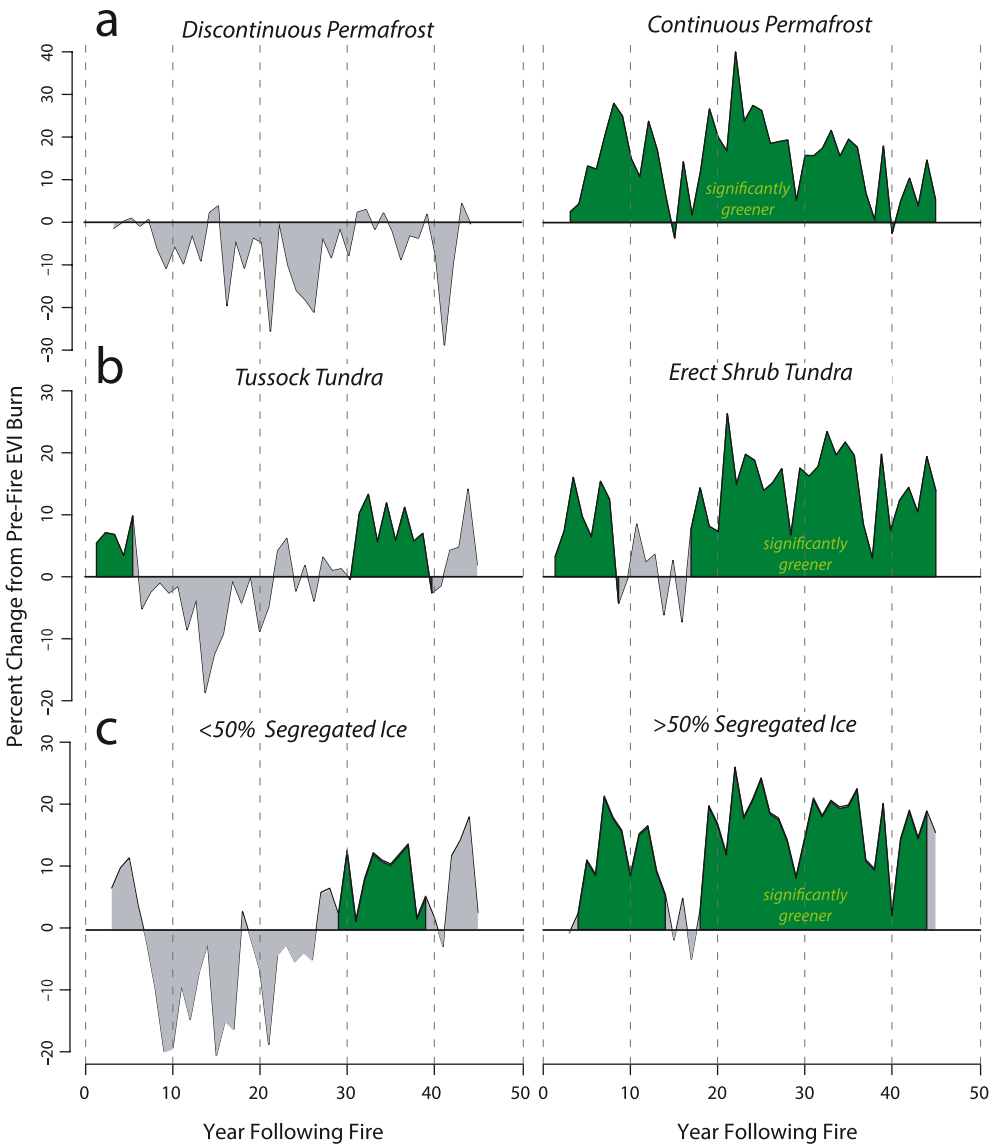

Figure 9. Percentage change of $EVI2_b$ relative to prefire values (5–1 year before fires) for burned terrain that varies in (a) permafrost type (Jorgenson et al., 2008) (b) vegetation type (Raynolds et al., 2019), and (c) percent segregated ice content (Jorgenson et al., 2014). Green polygons indicate when postfire $EVI2_b$ values are significantly greater than those 5–1 year before fires ($p < 0.05$).

tundra (Bret-Harte et al., 2013; Jiang et al., 2015; Wein & Bliss, 1973). The temporary nature of the first greening phase may be due to the rapid plant regrowth rates and higher nutrient runoff during the postfire recovery period, which eventually exhausts this initial postfire surplus of soil nutrients (Jiang et al., 2015; Larouche et al., 2015). Our results support the inference that the first greening phase is nutrient-fueled because it occurs at the most nutrient-limited sites, which often contain peat-producing plants, wet soils, and continuous permafrost. Overall, phase one of postfire greening is a widespread phenomenon, and, because postfire nutrient increases are common following fires (Knicker, 2007), the phenomenon of short-term, postfire greening will likely persist even as tundra fire regimes change in the future.

Phase two of postfire greening consists of a shift to an average ~14% greener land cover by ca. 16 years after fires (Figure 6d). We hypothesize this is caused by postfire shrub expansion facilitated by permafrost thaw. Evidence supporting this hypothesis includes: (1) It takes ca. 16 years for this greening phase to begin after fires, which roughly coincides with the time it took for annual growth rates of alder shrubs in

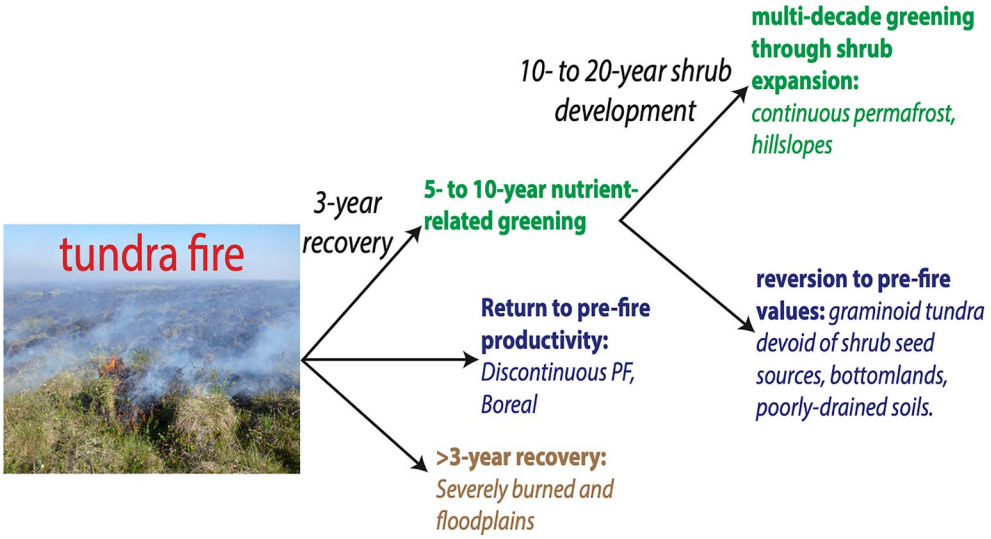

Figure 10. Timing and pathways of postfire tundra vegetation for different landscape situations in the Noatak watershed.

twice-burned areas to surpass alder growth rates in adjacent un-burned areas (ca. 13 years; Figures 6 and 8). This agreement between shrub ontogeny and remotely sensed vegetation data indicates that the onset of greening phase two is consistent with direct, albeit limited, measurements of postfire shrub expansion. (2) Phase two greening is confined to areas underlain by continuous permafrost, in areas where permafrost has an estimated >50% segregated ice content, and where sediment types are coarser and terrain is steeper (Figures 9 and S11). These are areas with abundant, near-surface ground ice that is likely to partially thaw after fire and coarse-textured soils that experience a shift to greater soil drainage after thaw. When thawed, this type of terrain experiences ground subsidence, and exposure of bare-soil patches, which are then available for plant establishment. As a consequence, these are also the areas of the landscape where warming-driven shrub expansion has been most pronounced over the last 80 years in the Noatak Valley and on the North Slope of Alaska (Tape et al., 2012). The spatial distribution of greening phase two supports the idea that significant permafrost thaw is often a prerequisite for persistent fire-induced vegetation greening (Jones et al., 2013, 2015; Liljedahl et al., 2007; Yi et al., 2009). Our results also suggest that postfire permafrost-thaw-induced greening occurs through postfire shrub expansion, which is captured in both our remote sensing record and dendrochronology results. (3) Finally, postfire greening phase two is minimal in tussock tundra where upright shrub seed sources are limited (Figure 9b). Having shrubs locally abundant before fires provides local seed sources and immediate postfire resprouting from unburned tissue. Overall, fires appear to enhance vegetation productivity for at least 45 years following fires, particularly in areas where thaw-induced shrub expansion occurs.

The timing and distribution of this two-phased greening pattern indicates that the negative feedbacks that organic soil surface horizons exert on vegetation change can be over come in situations where near-surface permafrost is vulnerable to thaw and soils are relatively well-drained. Tussock tundra is one fire-prone vegetation type where phase two of postfire greening is limited. The thick peat that helps maintain the cold, wet soils favorable for tussocks create conditions for a fire regime characterized by low-severity surface fires that do not typically affect the underlying permafrost. Part of the fire-insensitive features of tussock tundra involve the architecture of tussocks, which protect their vulnerable buds in a wet mass of old leaves and tillers. Another reason that tussock tundra seems to be inured to postfire greening is inter-tussock areas often harbor moss communities, which retain moisture and provide a significant insulative layer for the underlying permafrost. Our results suggest that the most paludified areas with wet sedge and tussock vegetation and/or with fine-grained sediments, and/or where permafrost thaw has already occurred (discontinuous permafrost zone), may not be as vulnerable to long-term permafrost and vegetation change until further warming and/or more severe burning occurs. Our findings suggest that the self-maintaining fire regime operating in tussock tundra rarely leads to significant long-term (decadal scale) changes in primary

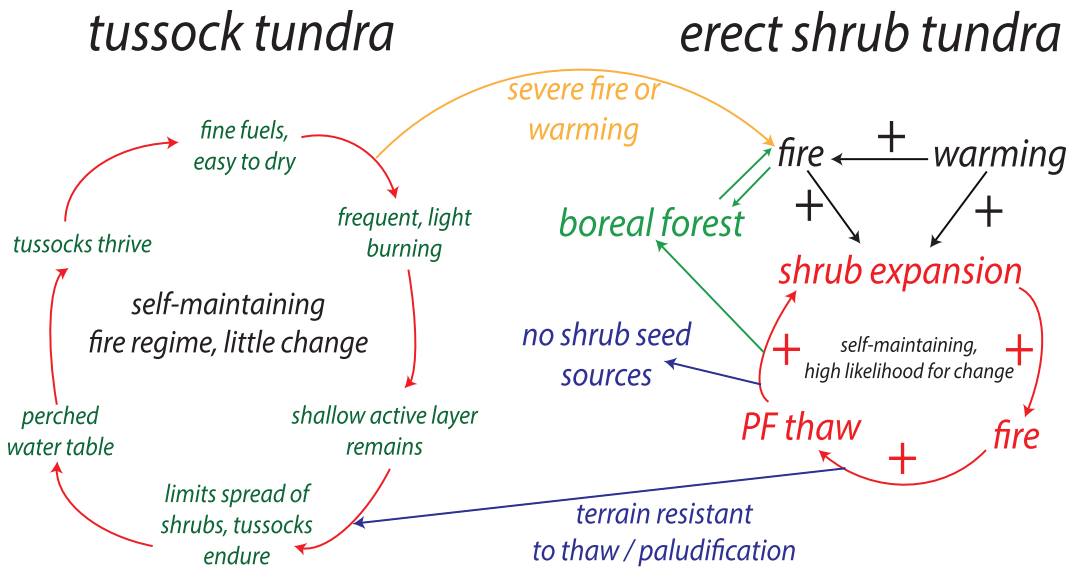

Figure 11. Two tundra fires regimes are operating simultaneously in the Noatak watershed. Tussock tundra communities possess a self-maintaining feedback loop that results in little vegetation change except in the most severely burned areas. In erect shrub tundra communities, a positive feedback likely maintains a fire regime where warming- or fire-driven shrub expansion leads to more severe burning and permafrost thaw, which then leads to enhanced greening and more fire. But there are several pathways out of this self-maintaining feedback loop that involve: (1) paludification when fire-free periods become unusually long, which can then lead back to tussock tundra, (2) areas where fire does not cause permafrost thaw, or where near-surface thaw has already reduced the amount of ground ice, and (3) areas where the seeds of shrubs (and/or trees) are unavailable. The self-maintaining properties of these feedbacks likely contribute to these two vegetation types being responsible for the 97% of the burned vegetation in the Noatak Valley.

productivity, and the vast majority of the non-shrubland tundra that burns, ends up in the fire-adapted tussock state. Due to the effects tundra fire regimes have on promoting this tussock vegetation type, we hypothesize that this will be an ecological attractor state that will become even more widespread when tundra fires become more frequent at higher latitudes (e.g., the North Slope of Alaska). Additional warming and greater burn severity of unknown magnitudes appear to be needed in order to shift tussock vegetation out of the negative feedback loops that tend to maintain them in their current state (Figures 10 and 11).

6.4. Noatak Tundra Fires as Net Greening Agents

Postfire greening over several decades eventually compensated for the reduced productivity observed in the first three years following tundra fires in the Noatak Valley. From an $EVI2_b$ perspective, tundra fires have enhanced cumulative primary productivity by 7% after the 44 years of postfire observation (Figure 6b). Because EVI2 is a surrogate for net ecosystem exchange in tundra regions (Rocha & Shaver, 2011), tundra fires in the Noatak may serve as agents of *net* carbon sequestration because postfire greening results in more productive vegetation than would have occurred if these areas went unburned. The cumulative $EVI2_b$ productivity index changed from negative to positive 22 years after fires, which suggests that tundra fires are greening agents only when fires occur at >22-year intervals. There is a growing concern that wildfire-derived carbon emissions will exacerbate global warming (Mack et al., 2011; Turetsky et al., 2015; Walker et al., 2019), which has led to proposals for suppressing Alaska's wildfires as one way to curtail greenhouse gas emissions (Grissom et al., 2000). Our results and those of postfire soil carbon assessments in Siberian tundra (Loranty et al., 2014) imply that these efforts must take into account postfire vegetation recovery and greening that could at least partially compensate for the losses of carbon during and after burning.

On the other hand, it would be premature to designate all tundra fires as climatic cooling agents because we have not taken into account the carbon losses from long-stored soil carbon that are not documented by the $EVI2_b$ index, (i.e., losses that could be caused by direct combustion or fire-induced permafrost thaw (Schädel et al., 2016; Schuur et al., 2009)). We stress, however, that such thaw-induced carbon release is

probably minimal after most fires in the Noatak Valley because the near-surface permafrost in the Late Pleistocene-glaciated terrain in the Noatak has a low carbon content. This is because much of the region was covered in valley glaciers and ice caps during most of the Pleistocene, so there were no plants contributing to soil organic matter (Hamilton, 2010; Kaufman et al., 2011).

Another important factor that we do not consider in this analysis is the land-surface feedback of postfire changes in albedo, which, initially after fire, has a localized warming effect that can change depending on postfire changes in vegetation cover (Beck et al., 2011; Pearson et al., 2013; Rocha et al., 2012). Another complication is posed by what types of greenhouse gases are emitted following a fire. Boreal and tundra fires have a tendency to change postfire drainage patterns and lead to changes in methane emissions (Köster et al., 2018). With these provisos in mind, our results suggest that in this relatively flammable Arctic region, tundra fires are unlikely to cause significant increases in net, long-term CO_2 emissions unless fires become exceptionally frequent (<22 years). More studies in more areas of the Arctic are needed to definitively answer the basic and important question of whether warming climate is changing tundra fire regimes in ways that cause a net loss or net gain of carbon to the atmosphere.

6.5. A Fire-Shrub-Greening Feedback Operating in Northwest Alaska's Tundra

We show that more productive, shrubbier areas burn more severely in the Noatak watershed and that tundra fires resulted in increased productivity and more shrub biomass. These results suggest that the negative feedbacks related to peat (soil organic horizons) in many parts of the Noatak Valley have limits and are susceptible to being pushed by fire and a warming climate across a critical threshold that leads either from tussock to shrubland communities, or, in the case of existing shrub communities to a denser shrub cover (Figures 10 and 11). The more severe burning supported by these shrublands likely prevents a return to a paludified steady state (as observed in Jones et al., 2013). Because of this ecological inertia, and because warming climate may be causing increased burning that is driving more sites towards this shrub-dominated community type, fire-prone erect shrub tundra is probably the other ecological attractor state that we should expect during the more fire-rich future of Arctic tundra. Because parts of the North Slope of Alaska and much of the circumpolar Low Arctic (<70°N) have similar vegetation and permafrost characteristics as the Noatak Valley, these regions may also be susceptible to similar regime shifts and the positive fire-shrub-greening feedback that we observe here. Based on these results, these shifts and feedbacks will be especially prevalent in areas where permafrost thaw leads to enhanced soil drainage and shrub expansion following fires (Frost et al., 2020; Jones et al., 2013; Lantz et al, 2010, 2013; Racine et al., 2006).

If the fire-shrub-greening feedback has been operating in the Noatak for some time, why is not the entire watershed covered by upright shrubland that burns severely? We suggest four ways that landscapes either avoid this ecological attractor state or escape from its feedback loop. First, even in a warming climate, fire is still a stochastic disturbance, and some places invariably go without fire for long periods of time. In these cases, undisturbed vegetation and organic-horizon buildup may proceed far enough to revert back to a paludified landscape where shrub expansion is curtailed and even reversed. Second, there are areas where the self-maintaining features of the tussock tundra fire regime prevent a shift into a different, shrub-reliant fire regime. In these cases, tussocks endure low-severity fires that kill off shrub competitors, and these sites remain in the tussock ecological attractor state. Third, due to fire-independent conditions related to surficial geology, ground-ice content, and soil, shrubs may be incapable of flourishing in some areas until more intense warming and/or greater burn severity occurs. Fourth, there is an exit pathway out of the fire-shrub-greening feedback that can occur in areas where an invasion of spruce trees ushers in a boreal forest fire regime. These possible exemptions to and exits from the fire-shrub-greening feedback loop should be considered when forecasting tundra fire regimes within a warming climate. The self-maintaining qualities of the shrub-greening and tussock-enduring maintenance fire regimes make up the two attractor states for flammable tundra in the Noatak, where they contribute to ~97% of burned area (Figure 11). Where and when tundra ecosystems enter and exit these attractor states will help determine the vegetation mosaic of the tundra biome in a warming Arctic.

7. Conclusions

We found that tundra fires occur in more productive vegetation types, and tundra plant communities in the Noatak watershed are highly resilient to fires. The resprouting of pre-fire plants and limited vegetation damage contribute to vegetation indices recovering to prefire values within about three years of burning. Satellite-derived vegetation productivity indices suggest that on a multi-decadal time scale (from 10 years before fires to 44 years after), tundra fires act to enhance the cumulative primary productivity by ~7% and thus act as a net greening agent. This fire-induced greening may act to partially offset a fire's climate-warming effects through greenhouse gas emissions and surface albedo changes following tundra fires, especially in cases where carbon-rich permafrost is not being thawed and ancient carbon is absent or evades combustion.

Postfire greening occurred in two stages. Phase one occurs between three and ten years after a fire in most plant community types, which we hypothesize is caused by a short-lived pulse in nutrient availability. The second phase of postfire greening is most likely to occur at sites where fire triggers near-surface permafrost thaw that leads to shrub expansion. The timing of this second stage of greening matches how long it takes shrub growth in thawed, burned areas to exceed growth in unburned and less-thawed areas.

A fire-shrub-greening positive feedback appears to be operating in much of the Noatak Valley. Shrubs yield more severe burning, which thaws permafrost and begets further shrub proliferation accompanied by warmer soils. This positive fire-shrub-greening feedback is limited by conditions that prevent postfire shrub expansion due to preexisting conditions related to soil, permafrost, and surficial geology, which have too-high a shrub-exclusion threshold for current climate warming and current fire regimes to cross. Theoretically, a warming-driven increase in the rate and severity of tundra burning *could* cause a regime shift from tussock tundra to tall shrub tundra, but this tussock-to-shrub regime shift appears to have been uncommon in the recent past, and both tussock tundra and erect shrub tundra fire regimes, which dominate the burned area in the Noatak, are operating somewhat independently via self-maintaining processes. Elsewhere, the fire-shrub-greening feedback is diverted to alternative states, as in areas that remain fire-free long enough to become paludified, or where boreal tree species become established after fires. Both the tussock and shrub fire-regime feedbacks have the potential to force fire-poor tundra into their separate attractor states as climate change makes fires more likely in tundra landscapes.

Acknowledgments
This project was funded by the Joint Fire Science Program (Project 16-1-01-8 awarded to D. H. Mann and B. V. Gaglioti), and the National Science Foundation Arctic Natural Sciences program (16-61723 awarded to L. Andreu-Hayles, R. D. D'Arrigo, and S. J. Goetz). B. V. Gaglioti was partially funded by the Lamont-Doherty Earth Observatory's Postdoctoral Fellowship Program. L. Andreu-Hayles was partially funded by National Science Foundation grant PLR-1504134. S. J. Goetz, L. T. Berner, and K. Orndahl were supported by the NASA Arctic Boreal Vulnerability Experiment (grants NNX17AE44G and 80NSSC19M0112 to S. J. Goetz). B. M. Jones was supported by the National Science Foundation Office of Integrative Activities (OIA-1929170) programs. The authors thank Louise Farquharson for providing permafrost modeling results presented in Figure 1. We also thank Virgil E. Purchase for fieldwork, Golden Eagle Flight Service for expert piloting, and Kyle Hansen for measuring and cross-dating Alder ramets. Our thinking about this subject benefitted from discussions with Eric Miller and Jennifer Barnes. This is LDEO contribution #8480.

Data Availability Statement

Upon acceptance, the data that contributed to this paper will be available in open access data repositories. The dendrochronology data will be housed at NOAA Paleoclimatology database in the following locations: Ring Widths Once-Burned Site (https://www.ncdc.noaa.gov/paleo-search/study/32562) Ring Widths Twice-Burned Site (https://www.ncdc.noaa.gov/paleo-search/study/32563); Ring Widths Unburned Site (https://www.ncdc.noaa.gov/paleo-search/study/32564).

The remote sensing data will be housed at the NSF Arctic Data Center (https://arcticdata.io/catalog/view/doi%3A10.18739%2FA2DV1CP69).

References

AICC (Alaska Interagency Coordination Center) (2019). *Alaska historical fire information*. Retrieved from https://afsmaps.blm.gov/imf_firehistory/imf.jsp?site=firehistory

Andreu-Hayles, L., Gaglioti, B. V., Berner, L. T., Levesque, M., Anchukaitis, K. J., Goetz, S. J., & D'Arrigo, R. D. (2020). A narrow window of summer temperatures associated with shrub growth in Arctic Alaska. *Environmental Research Letters*, *15*(10), 105012

Barrett, K., Rocha, A. V., van de Weg, M. J., & Shaver, G. (2012). Vegetation shifts observed in arctic tundra 17 years after fire. *Remote Sensing Letters*, *3*(8), 729–736. https://doi.org/10.1080/2150704x.2012.676741

Baughman, C. A., Mann, D. H., Verbyla, D. L., & Kunz, M. L. (2015). Soil surface organic layers in Arctic Alaska: Spatial distribution, rates of formation, and microclimatic effects. *Journal of Geophysical Research: Biogeosciences*, *120*(6), 1150–1164. https://doi.org/10.1002/2015jg002983

Beck, P. S., Goetz, S. J., Mack, M. C., Alexander, H. D., Jin, Y., Randerson, J. T., & Loranty, M. (2011). The impacts and implications of an intensifying fire regime on Alaskan boreal forest composition and albedo. *Global Change Biology*, *17*(9), 2853–2866. https://doi.org/10.1111/j.1365-2486.2011.02412.x

Berner, L. T., Jantz, P., Tape, K. D., & Goetz, S. J. (2018). Tundra plant above-ground biomass and shrub dominance mapped across the North Slope of Alaska. *Environmental Research Letters*, *13*(3), 035002. https://doi.org/10.1088/1748-9326%2Faaaa9a

Berner, L. T., Massey, R., Jantz, P., Forbes, B. C., Macias-Fauria, M., Myers-Smith, I., et al. (2020). Summer warming explains widespread but not uniform greening in the Arctic tundra biome. *Nature Communications*, *11*(1), 1–12. https://doi.org/10.1038/s41467-020-18479-5

Biondi, F. (1999). Comparing tree-ring chronologies and repeated timber inventories as forest monitoring tools. *Ecological Applications*, *9*(1), 216–227.

Bret-Harte, M. S., Mack, M. C., Shaver, G. R., Huebner, D. C., Johnston, M., Mojica, C. A., et al. (2013). The response of Arctic vegetation and soils following an unusually severe tundra fire. *Philosophical Transactions of the Royal Society B: Biological Sciences*, *368*(1624), 20120490. https://doi.org/10.1098/rstb.2012.0490

Chapin, F. S., & Starfield, A. M. (1997). Time lags and novel ecosystems in response to transient climatic change in Arctic Alaska. *Climatic Change*, *35*(4), 449–461.

Chapin, F. S., III, van Cleve, K., & Chapin, M.C. (1979). Soil temperature and nutrient cycling in the tussock growth form of *Eriophorum vaginatum*. *Journal of Ecology*, *67*(1), 169–189.

Chipman, M., Hudspith, V., Higuera, P., Duffy, P., Kelly, R., Oswald, W., & Hu, F. S. (2015). Spatiotemporal patterns of tundra fires: Late-Quaternary charcoal records from Alaska. *Biogeosciences*, *12*(13), 4017–4027. https://doi.org/10.5194/bg-12-4017-2015

Fetcher, N., & Shaver, G. (1983). Life histories of tillers of *Eriophorum vaginatum* in relation to tundra disturbance. *Journal of Ecology*, *71*(1), 131–147.

Folke, C., Carpenter, S., Walker, B., Scheffer, M., Elmqvist, T., Gunderson, L., & Holling, C. S. (2004). Regime shifts, resilience, and biodiversity in ecosystem management. *Annual Review of Ecology, Evolution, and Systematics*, *35*(1), 557–581. https://doi.org/10.1146/annurev.ecolsys.35.021103.105711

French, N. H., Jenkins, L. K., Loboda, T. V., Flannigan, M., Jandt, R., Bourgeau-Chavez, L. L., & Whitley, M. (2015). Fire in arctic tundra of Alaska: Past fire activity, future fire potential, and significance for land management and ecology. *International Journal of Wildland Fire*, *24*(8), 1045–1061. https://doi.org/10.1071/wf14167

Frost, G. V., Loehman, R. A., Saperstein, L. B., Macander, M. J., Nelson, P. R., Paradis, D. P., & Natali, S. M. (2020). Multi-decadal patterns of vegetation succession after tundra fire on the Yukon-Kuskokwim Delta, Alaska. *Environmental Research Letters*, *15*(2), 025003. https://doi.org/10.1088/1748-9326/ab5f49

Gaglioti, B. V., Mann, D. H., Jones, B. M., Wooller, M. J., & Finney, B. P. (2016). High-resolution records detect human-caused changes to the boreal forest wildfire regime in interior Alaska. *The Holocene*, *26*(7), 1064–1074. https://doi.org/10.1177/0959683616632893

Gibson, C. M., Chasmer, L. E., Thompson, D. K., Quinton, W. L., Flannigan, M. D., & Olefeldt, D. (2018). Wildfire as a major driver of recent permafrost thaw in boreal peatlands. *Nature Communications*, *9*(1), 1–9. https://doi.org/10.1038/s41467-018-05457-1

Gibson, C. M., Estop-Aragonés, C., Flannigan, M., Thompson, D. K., & Olefeldt, D. (2019). Increased deep soil respiration detected despite reduced overall respiration in permafrost peat plateaus following wildfire. *Environmental Research Letters*, *14*(12), 125001. https://doi.org/10.1088/1748-9326/ab4f8d

Gorelick, N., Hancher, M., Dixon, M., Ilyushchenko, S., Thau, D., & Moore, R. (2017). Google Earth Engine: Planetary-scale geospatial analysis for everyone. *Remote Sensing of Environment*, *202*(1), 18–27. https://doi.org/10.1016/j.rse.2017.06.031

Grissom, P., Alexander, M. E., Cella, B., Cole, F., Kurth, J. T., Malotte, N. P., et al. (2000). *Effects of climate change on management and policy: Mitigation options in the* (pp. 85–101). North American boreal forest.

Hall, D., Brown, J., & Johnson, L. (1978). The 1977 tundra fire at Kokolik River, Alaska. *Arctic*. *31*,1.

Hamilton, T. D. (2009). *Guide to surficial geology and river-bluff exposures, Noatak National Preserve, northwestern Alaska*. US Geological Survey.

Hamilton, T. D. (2010). *Surficial geologic map of the Noatak National Preserve, Alaska*.US Geological Survey.

Hansen, M. C., Potapov, P. V., Moore, R., Hancher, M., Turubanova, S. A., Tyukavina, A., et al. (2013). High-resolution global maps of 21st-century forest cover change. *Science*, *342*(6160), 850–853. https://doi.org/10.1126/science.1244693

Heim, R. J., Bucharova, A., Rieker, D., Yurtaev, A., Kamp, J., & Hölzel, N. (2019). *Long-term effects of fire on Arctic tundra vegetation in Western Siberia* (p. 756163). BioRxiv.

Higuera, P. E., Brubaker, L. B., Anderson, P. M., Brown, T. A., Kennedy, A. T., & Hu, F. S. (2008). Frequent fires in ancient shrub tundra: Implications of paleorecords for arctic environmental change. *PloS One*, *3*(3), e0001744. https://doi.org/10.1371/journal.pone.0001744

Higuera, P. E., Brubaker, L. B., Anderson, P. M., Hu, F. S., & Brown, T. A. (2009). Vegetation mediated the impacts of postglacial climate change on fire regimes in the south-central Brooks Range, Alaska. *Ecological Monographs*, *79*(2), 201–219. https://doi.org/10.1890/07-2019.1

Higuera, P. E., Chipman, M. L., Barnes, J. L., Urban, M. A., & Hu, F. S. (2011). Variability of tundra fire regimes in Arctic Alaska: Millennial-scale patterns and ecological implications. *Ecological Applications*, *21*(8), 3211–3226. https://doi.org/10.1890/11-0387.1

Hinzman, L., Kane, D., Gieck, R., & Everett, K. (1991). Hydrologic and thermal properties of the active layer in the Alaskan Arctic. *Cold Regions Science and Technology*, *19*(2), 95–110.

Holmes, R. L. (1983). Computer-assisted quality control in tree-ring dating and measurement. *Tree-Ring Bulletin*, *43*(1), 69–78.

Horel, J. D., & Dong, X. (2010). An evaluation of the distribution of Remote Automated Weather Stations (RAWS). *Journal of Applied Meteorology and Climatology*, *49*(7), 1563–1578. https://doi.org/10.1175/2010jamc2397.1

Hu, F. S., Higuera, P. E., Duffy, P., Chipman, M. L., Rocha, A. V., Young, A. M., et al. (2015). Arctic tundra fires: natural variability and responses to climate change. *Frontiers in Ecology and the Environment*, *13*(7), 369–377. https://doi.org/10.1890/150063

Hu, F. S., Higuera, P. E., Walsh, J. E., Chapman, W. L., Duffy, P. A., Brubaker, L. B., & Chipman, M. L. (2010). Tundra burning in Alaska: Linkages to climatic change and sea ice retreat. *Journal of Geophysical Research: Biogeosciences*, *115*(G4). https://doi.org/10.1029/2009jg001270

Jandt, R., Miller, E., Yokel, D., Bret-Harte, M., Mack, M., & Kolden, C. (2012). *Findings of Anaktuvuk River fire recovery study*. Fairbanks, AK: US Department of Interior Bureau of Land Management.

Jiang, Y., Rastetter, E. B., Rocha, A. V., Pearce, A. R., Kwiatkowski, B. L., & Shaver, G. R. (2015). Modeling carbon–nutrient interactions during the early recovery of tundra after fire. *Ecological Applications*, *25*(6), 1640–1652. https://doi.org/10.1890/14-1921.1

Jiang, Z., Huete, A. R., Didan, K., & Miura, T. (2008). Development of a two-band enhanced vegetation index without a blue band. *Remote Sensing of Environment*, *112*(10), 3833–3845. https://doi.org/10.1016/j.rse.2008.06.006

Johnstone, J. F., & Chapin, F. S. (2006). Effects of soil burn severity on post-fire tree recruitment in boreal forest. *Ecosystems*, *9*(1), 14–31. https://doi.org/10.1007/s10021-004-0042-x

Jones, B. M., Breen, A. L., Gaglioti, B. V., Mann, D. H., Rocha, A. V., Grosse, G., et al. (2013). Identification of unrecognized tundra fire events on the north slope of Alaska. *Journal of Geophysical Research: Biogeosciences*, *118*(3), 1334–1344. https://doi.org/10.1002/jgrg.20113

Jones, B. M., Grosse, G., Arp, C. D., Miller, E., Liu, L., Hayes, D. J., & Larsen, C. F. (2015). Recent Arctic tundra fire initiates widespread thermokarst development. *Scientific Reports*, *5*, 15865.(1), https://doi.org/10.1038/srep15865

Jones, B. M., Kolden, C. A., Jandt, R., Abatzoglou, J. T., Urban, F., & Arp, C. D. (2009). Fire behavior, weather, and burn severity of the 2007 Anaktuvuk River tundra fire, North Slope, Alaska. *Arctic, Antarctic, and Alpine Research*, *41*(3), 309–316. https://doi.org/10.1657/1938-4246-41.3.309

Jorgenson, M. T., Kanevskiy, M., Shur, Y., Grunblatt, J., Ping, C. L, & Michaelson, G. (2014). *Permafrost database development, characterization, and mapping for northern Alaska*, Fairbanks, Alaska: Arctic Landscape Conservation Cooperative. Retrieved from https://scholarworks.alaska.edu/handle/11122/10373

Kaufman, D. S., Young, N. E., Briner, J. P., & Manley, W. F. (2011). Alaska palaeo-glacier atlas (version 2). *Developments in Quaternary Sciences*, (Vol. 15, pp. 427–445). Elsevier.

Knicker, H. (2007). How does fire affect the nature and stability of soil organic nitrogen and carbon? A review. *Biogeochemistry*, *85*(1), 91–118. https://doi.org/10.1007/s10533-007-9104-4

Köster, E., Köster, K., Berninger, F., Prokushkin, A., Aaltonen, H., Zhou, X., & Pumpanen, J. (2018). Changes in fluxes of carbon dioxide and methane caused by fire in Siberian boreal forest with continuous permafrost. *Journal of Environmental Management*, *228*(1), 405–415. https://doi.org/10.1016/j.jenvman.2018.09.051

Landhausser, S. M., & Wein, R. W. (1993). Postfire vegetation recovery and tree establishment at the Arctic treeline: Climate-change-vegetation-response hypotheses. *Journal of Ecology*, *81*(4), 665–672.

Lantz, T. C., Gergel, S. E., & Henry, G. H. (2010). Response of green alder (*Alnus viridis* subsp. *fruticosa*) patch dynamics and plant community composition to fire and regional temperature in north-western Canada. *Journal of Biogeography*, *37*(8), 1597–1610. https://doi.org/10.1007/s10021-012-9595-2

Lantz, T. C., Marsh, P., & Kokelj, S. V. (2013). Recent shrub proliferation in the Mackenzie Delta uplands and microclimatic implications. *Ecosystems*, *16*(1), 47–59. https://doi.org/10.1007/s10021-012-9595-2

Larouche, J. R., Abbott, B. W., Bowden, W. B., & Jones, J. B. (2015). The role of watershed characteristics, permafrost thaw, and wildfire on dissolved organic carbon biodegradability and water chemistry in Arctic headwater streams. *Biogeosciences Discussions*, *12*(5), 4221–4233. https://doi.org/10.5194/bg-12-4221-2015

Liljedahl, A., Hinzman, L., Busey, R., & Yoshikawa, K. (2007). Physical short-term changes after a tussock tundra fire, Seward Peninsula, Alaska. *Journal of Geophysical Research: Earth Surface*, *112*(F2). https://doi.org/10.1029/2006jf000554

Loboda, T., Chen, D., Hall, J., & He, J. (2018). *ABoVE: Landsat-derived Burn Scar dNBR across Alaska and Canada, 1985-2015*. ORNL DAAC.

Loranty, M. M., Abbott, B. W., Blok, D., Douglas, T. A., Epstein, H. E., Forbes, B. C., et al. (2018). Reviews and syntheses: Changing ecosystem influences on soil thermal regimes in northern high-latitude permafrost regions. *Biogeosciences*, *15*(17), 5287–5313. https://doi.org/10.5194/bg-15-5287-2018

Loranty, M. M., Natali, S. M., Berner, L. T., Goetz, S. J., Holmes, R. M., Davydov, S. P., et al. (2014). Siberian tundra ecosystem vegetation and carbon stocks four decades after wildfire. *Journal of Geophysical Research: Biogeosciences*, *119*(11), 2144–2154. https://doi.org/10.1002/2014jg002730

Mack, M. C., Bret-Harte, M. S., Hollingsworth, T. N., Jandt, R. R., Schuur, E. A., Shaver, G. R., & Verbyla, D. L. (2011). Carbon loss from an unprecedented Arctic tundra wildfire. *Nature*, *475*(7357), 489–492. https://doi.org/10.1038/nature10283

Marchenko, S., Romanovsky, V., & Tipenko, G. (2008). Numerical modeling of spatial permafrost dynamics in Alaska. Proceedings of the ninth international conference on permafrost(Vol. 29, pp. 1125–1130). Institute of Northern Engineering, University of Alaska Fairbanks.

Martin, A. C., Jeffers, E., Petrokofsky, G., Myers-Smith, I., & Macias-Fauria, M. (2017). Shrub growth and expansion in the Arctic tundra: An assessment of controlling factors using an evidence-based approach. *Environmental Research Letters*, *12*(8), 085007. https://doi.org/10.1038/nature10283

Masek, J. G., Vermote, E. F., Saleous, N. E., Wolfe, R., Hall, F. G., Huemmrich, K. F., et al. (2006). A Landsat surface reflectance dataset for North America, 1990–2000. *IEEE Geoscience and Remote Sensing Letters*, *3*(1), 68–72. https://doi.org/10.1109/lgrs.2005.857030

Masrur, A., Petrov, A. N., & DeGroote, J. (2018). Circumpolar spatio-temporal patterns and contributing climatic factors of wildfire activity in the Arctic tundra from 2001–2015. *Environmental Research Letters*, *13*(1), 014019. https://doi.org/10.1088/1748-9326/aa9a76

Myers-Smith, I. H., Forbes, B. C., Wilmking, M., Hallinger, M., Lantz, T., Blok, D., et al. (2011). Shrub expansion in tundra ecosystems: Dynamics, impacts and research priorities. *Environmental Research Letters*, *6*(4), 045509. https://doi.org/10.1088/1748-9326/6/4/045509

Myers-Smith, I. H., Kerby, J. T., Phoenix, G. K., Bjerke, J. W., Epstein, H. E., Assmann, J. J., et al. (2020). Complexity revealed in the greening of the Arctic. *Nature Climate Change*, *10*(2), 106–117. https://doi.org/10.1038/s41558-019-0688-1

Pearson, R. G., Phillips, S. J., Loranty, M. M., Beck, P. S. A., Damoulas, T., Knight, S. J., & Goetz, S. J. (2013). Shifts in Arctic vegetation and associated feedbacks under climate change. *Nature Climate Change*, *3*(7), 673–677. https://doi.org/10.1038/nclimate1858

Racine, C., Allen, J. L., & Dennis, J. G. (2006). *Long-term monitoring of vegetation change following tundra fires in Noatak National Preserve, Alaska*. Fairbanks, Alaska, USA: Arctic Network of Parks Inventory and Monitoring Program, National Park Service, Alaska Region.

Racine, C., Jandt, R., Meyers, C., & Dennis, J. (2004). Tundra fire and vegetation change along a hillslope on the Seward Peninsula, Alaska, USA. *Arctic, Antarctic, and Alpine Research*, *36*(1), 1–10. https://doi.org/10.1657/1523-0430(2004)036[0001:tfavca]2.0.co;2

Racine, C. H. (1981). Tundra fire effects on soils and three plant communities along a hill-slope gradient in the Seward Peninsula, Alaska. *Arctic*, *34*(1), 71–84.

Racine, C. H., Dennis, J. G., & Patterson, W. A., III (1985). Tundra fire regimes in the Noatak River watershed, Alaska: 1956-83. *Arctic*, *38*(3), 194–200.

Racine, C. H., Johnson, L. A., & Viereck, L. A. (1987). Patterns of vegetation recovery after tundra fires in northwestern Alaska, USA. *Arctic and Alpine Research*, *19*(4), 461–469.

Rahman, A., Sims, D. A., Cordova, V. D., & El-Masri, B. Z. (2005). Potential of MODIS and surface temperature for directly estimating per-pixel ecosystem C fluxes. *Geophysical Research Letters*, *32*(19). https://doi.org/10.1029/2005gl024127

Raynolds, M.K., Walker, D.A., Balser, A., Bay, C., Campbell, M., Cherosov, M.M., et al. (2019). A raster version of the Circumpolar Arctic Vegetation Map (CAVM). *Remote Sensing of Environment*, *232*, 111297.(1), https://doi.org/10.1016/j.rse.2019.111297

Rocha, A. V., Loranty, M. M., Higuera, P. E., Mack, M. C., Hu, F. S., Jones, B. M., et al. (2012). The footprint of Alaskan tundra fires during the past half-century: Implications for surface properties and radiative forcing. *Environmental Research Letters*, *7*(4), 044039. https://doi.org/10.1088/1748-9326/7/4/044039

Rocha, A. V., & Shaver, G. R. (2009). Advantages of a two band calculated from solar and photosynthetically active radiation fluxes. *Agricultural and Forest Meteorology*, *149*(9), 1560–1563. https://doi.org/10.1016/j.agrformet.2009.03.016

Rocha, A. V., & Shaver, G. R. (2011). Burn severity influences postfire CO_2 exchange in arctic tundra. *Ecological Applications*, *21*(2), 477–489. https://doi.org/10.1890/10-0255.1

Schädel, C., Bader, M. K.-F., Schuur, E. A., Biasi, C., Bracho, R., Čapek, P., et al. (2016). Potential carbon emissions dominated by carbon dioxide from thawed permafrost soils. *Nature Climate Change*, *6*(10), 950–953. https://doi.org/10.1038/nclimate3054

Schuur, E. A., Vogel, J. G., Crummer, K. G., Lee, H., Sickman, J. O., & Osterkamp, T. (2009). The effect of permafrost thaw on old carbon release and net carbon exchange from tundra. *Nature*, *459*(7246), 556–559. https://doi.org/10.1038/nature08031

Shilts, W. W. (1978). Nature and genesis of mudboils, central Keewatin, Canada. *Canadian Journal of Earth Sciences*, *15*(7), 1053–1068.

Smith, S., Romanovsky, V., Lewkowicz, A., Burn, C. R., Allard, M., Clow, G., et al. (2010). Thermal state of permafrost in North America: A contribution to the international polar year. *Permafrost and Periglacial Processes*, *21*(2), 117–135. https://doi.org/10.1002/ppp.690

Stokes, M. A. (1996). *An introduction to tree-ring dating*. University of Arizona Press.

Tape, K., Sturm, M., & Racine, C. (2006). The evidence for shrub expansion in Northern Alaska and the Pan-Arctic. *Global Change Biology*, *12*(4), 686–702. https://doi.org/10.1111/j.1365-2486.2006.01128.x

Tape, K. D., Hallinger, M., Welker, J. M., & Ruess, R.W. (2012). Landscape heterogeneity of shrub expansion in Arctic Alaska. *Ecosystems*, *15*(5), 711–724. https://doi.org/10.1007/s10021-012-9540-4

Tsuyuzaki, S., Iwahana, G., & Saito, K. (2018). Tundra fire alters vegetation patterns more than the resultant thermokarst. *Polar Biology*, *41*(4), 753–761. https://doi.org/10.1007/s00300-017-2236-7

Turetsky, M., Donahue, W. F., & Benscoter, B. (2011). Experimental drying intensifies burning and carbon losses in a northern peatland. *Nature Communications*, *2*(1), 1–5. https://doi.org/10.1038/ncomms1523

Turetsky, M. R., Benscoter, B., Page, S., Rein, G., van der Werf, G. R., & Watts, A. (2015). Global vulnerability of peatlands to fire and carbon loss. *Nature Geoscience*, *8*(1), 11–14. https://doi.org/10.1038/ngeo2325

Vavrek, M. C., Fetcher, N., McGraw, J. B., Shaver, G., Chapin, F. S., III, & Bovard, B. (1999). Recovery of productivity and species diversity in tussock tundra following disturbance. *Arctic, Antarctic, and Alpine Research*, *31*(3), 254–258.

Vermote, E., Justice, C., Claverie, M., & Franch, B. (2016). Preliminary analysis of the performance of the Landsat 8/OLI land surface reflectance product. *Remote Sensing of Environment*, *185*(1), 46–56. https://doi.org/10.1016/j.rse.2016.04.008

Walker, X. J., Baltzer, J. L., Cumming, S. G., Day, N. J., Ebert, C., Goetz, S., et al. (2019). Increasing wildfires threaten historic carbon sink of boreal forest soils. *Nature*, *572*(7770), 520–523. https://doi.org/10.1038/s41586-019-1474-y

Wein, R. W., & Bliss, L. C. (1973). Changes in arctic Eriophorum tussock communities following fire. *Ecology*, *54*(4), 845–852.

Wein, R. W., & Shilts, W. (1976). *Tundra fires in the District of Keewatin* (pp. 511–515). Geological Survey of Canada, Paper.

Yi, S., McGuire, A. D., Harden, J., Kasischke, E., Manies, K., Hinzman, L., et al. (2009). Interactions between soil thermal and hydrological dynamics in the response of Alaska ecosystems to fire disturbance. *Journal of Geophysical Research: Biogeosciences*, *114*(G2). https://doi.org/10.1029/2008jg000841

Yi, S., Woo, M., & Arain, M. A. (2007). Impacts of peat and vegetation on permafrost degradation under climate warming. *Geophysical Research Letters*, *34*(16). https://doi.org/10.1029/2007gl030550